

**Estimation of Shrinkage and Dimensional Inaccuracy in Typical Surfaces Produces by
FDM**

A Dissertation submitted in partial fulfilment of the requirement for the degree of

Master of Engineering

In

CAD/CAM Engineering

By

Ish Kumar Rumpaul

801684005

Under the Supervision of

Dr. Vineet Srivastava

(Assistant Professor, Mechanical Engineering Department)



THAPAR INSTITUTE
OF ENGINEERING & TECHNOLOGY
(Deemed to be University)

**MECHANICAL ENGINEERING DEPARTMENT
THAPAR INSTITUTE OF ENGINEERING AND TECHNOLOGY, PATIALA
JUNE 2018**

CERTIFICATE

This is to clarify that the work done in this thesis report title "**Estimation of Shrinkage and Dimensional Inaccuracy in Typical Surfaces Produces by FDM**" submitted in partial fulfilment of required award of Master of Engineering in CAD/CAM in the Mechanical Engineering department of TIET, Patiala, is an authentic record of work carried by me under the guidance of Dr. Vineet Srivastava, Assistant Professor Mechanical Engineering department, TIET, Patiala. The embodied in this report has not been submitted by in any part or full to any other university or institute for the award of any degree.

Date 9/8/18

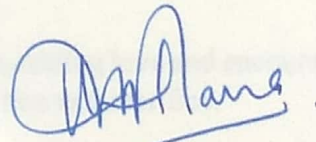


Ish Kumar Rumpaul

Roll No: 801684005

This is to certify that above declaration made by the student concerned is correct to the best of my knowledge & belief.

Date 09/08/2018



Dr. Vineet Srivastava

Assistant Professor

Mechanical Engineering Department

TIET, Patiala

Acknowledgment

There are few people that I would like specially to acknowledge and extend my heartfelt gratitude who have made the completion of this report possible. With the biggest contribution to this report, I would like to thank Dr. Vineet Srivastava who have guided me with his full support with stimulating suggestions and encouragement to go ahead in all time of report.

I am also thankful to Dr. Tejinder Paul Singh, Professor and Head, Mechanical Engineering Department, for permitting us with adequate infrastructure for carrying out the work.

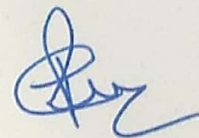
I am also thankful to Dr Pulak M. Pandey, Professor IIT Delhi for permitting to conduct experimental test in Rapid Prototyping Laboratory, IIT Delhi.

I am also thankful to Mr. Gurminder Singh, Research Scholar, Mechanical Engineering Department, IIT Delhi for his help in conducting tests in Rapid Prototyping Laboratory.

I am also thankful to Mr. Narinder Singh, Associate Lab, Mechanical Engineering Department for his help in conducting experimental tests in Advanced Measurement Lab.

I am also thankful to Dr. J S Saini, P.G. Coordinator, Mechanical Engineering Department.

Lastly, I would like to thank my parents for their years of unyielding love and encourage. They always wanted the best for me and I admire their determination and sacrifice.



Ish Kumar Rumpaul

Contents

CERTIFICATE	II
ACKNOWLEDGMENT	III
LIST OF FIGURES	VI
LIST OF TABLES	VIII
ABSTRACT	IX
CHAPTER 1: INTRODUCTION	1
1.1 Rapid Prototyping	1
1.2 Historical Development of Rapid Prototyping	2
1.3 Types of Rapid Prototyping System	3
1.4 Process Planning in Rapid Prototyping	9
CHAPTER 2: LITERATURE REVIEW	12
2.1 Risk Factors/Uncertainties/Possible Sources of Error	12
2.2 Studies related to the Accuracy and Strength of the Part	13
2.3 Gap in Literature	16
2.4 Research Objectives	16
CHAPTER 3: PLANNING OF EXPERIMENT	18
3.1 FDM Process	18
3.2 Material Properties	21
3.3 Mean Method	22
3.4 CMM	23
3.5 Selection of Typical Surfaces	23
3.6 Fabrication of Surfaces	24
3.7 Measurement of Aluminium Models	27
3.8 CAD Modeling	31

3.9 Part Fabrication in FDM	32
3.10 Study of Shrinkage	33
CHAPTER 4: REVERSE ENGINEERING	38
4.1 Methodology	39
4.2 Data Collection from Physical Part	39
4.3 Principle of 3D Scanner	40
4.4 Generation of Parts	41
4.5 Fabrication of Reverse Engineered Part	43
CHAPTER 5: COMPARATIVE ANALYSIS OF SHRINKAGE FOR PARTS	45
5.1 Comparison of Various Parts	45
5.2 Designing of Shrinkage Compensation Factor	50
5.3 Fabrication of Parts Containing SCF	51
5.4 Dimensional Analysis of Parts Containing SCF	52
5.5 Statistical Modelling of Shrinkage for X Direction Laying	55
CONCLUSIONS	56
FUTURE SCOPE	60
REFERENCES	61
WEB REFERENCES	64
ANNEXURE 1	65
ANNEXURE 2	81

List of Figures

Figure 1.1: Stereolithography	4
Figure 1.2: Selective Laser Sintering.....	5
Figure 1.3: Laminated Object Manufacturing	6
Figure 1.4: Laser Engineering Net Shaping.....	7
Figure 1.5: 3D Printing	7
Figure 1.6 Fused Deposition Modeling	8
Figure 1.7: Rapid Prototyping Process Chain.....	9
Figure 1.8: Curling of Parts	10
Figure 1.9: Stair Stepping	11
Figure 3.1: Stratasys uPrint SE	19
Figure 3.2: Layer by layer deposition in Z direction	19
Figure 3.3: Extruders of FDM Machine	20
Figure 3.4: Build Platform	20
Figure 3.5: Infill Pattern.....	21
Figure 3.6: Orientation of Part	21
Figure 3.7: Co-ordinate Measuring Machine.....	23
Figure 3.8: Four Selected Surfaces	24
Figure 3.9: Fabrication of Parts	26
Figure 3.10: Parts Fabricated by VMC	27
Figure 3.11: Spectra CMM	28
Figure 3.12: Part (A).....	28
Figure 3.13: Part (B)	29
Figure 3.14: Part (C)	30
Figure 3.15: Part (D).....	31
Figure 3.16: CAD Models.....	32
Figure 3.17: Process Parameters in FDM	33
Figure 3.18: Part Produced by FDM.....	33
Figure 3.19: ABS Part (A)	34
Figure 3.20: ABS Part (B)	35
Figure 3.21: ABS Part (B)	36
Figure 3.22: ABS Part (D)	36
Figure 4.1: Forward Engineering.....	38
Figure 4.2: Reverse Engineering.....	38
Figure 4.3: Reverse Engineering Methodology	39
Figure 4.4: Principle of 3D Scanner	41
Figure 4.5: 3 D Scanner	42
Figure 4.6: Point Cloud Files	43
Figure 4.7: Fabrication of Reverse Engineered Part.....	43
Figure 5.1: Dimensional Analysis of Part (A)	46
Figure 5.2 Dimensional Analysis of Part (B).....	47
Figure 5.3 Dimensional Analysis of Part (C).....	48
Figure 5.4 Dimensional Analysis of Part (D)	49
Figure 5.5: Comparison of Part A.....	52
Figure 5.6: Comparison of Part B.....	53

Figure 5.7: Comparison of Part C.....	54
Figure 5.8: Comparison of Part D.....	55
Figure 5.9: Main effect plot for shrinkage along the length in x direction.....	56
Figure 5.10: Response Surfaces for shrinkage for x direction laying along the length.....	56
Figure 5.11: Main effect plot for shrinkage along the width in x direction laying.....	57
Figure 5.12: Response Surfaces for shrinkage for x direction laying along the width.....	57
Figure 5.13: Response Surfaces for shrinkage for x direction laying along the Height.....	58
Figure 5.14: Response Surfaces for shrinkage for x direction laying along the Height.....	58

List of Tables

Table 1.1: Growth of Rapid Prototyping and Similar Systems	2
Table 3.1: Properties of ABS-M30	22
Table 3.2: Specification of VMC.....	25
Table 3.3: Dimensions of Part (A).....	29
Table 3.4: Dimensions of Part (B)	29
Table 3.5: Dimensions of Part (C)	30
Table 3.6: Dimensions of Part (D).....	31
Table 3.7: Dimensions of ABS Part (A)	34
Table 3.8: Dimensions of ABS Part (B)	35
Table 3.9: Dimensions of ABS Part (C)	36
Table 3.10: Dimensions of ABS Part (D).....	37
Table 5.1: Mean of Change in Length of Parts.....	50
Table 5.2: Mean of Change in Breadth of Parts.....	51
Table 5.3: Mean of Change in Height of Parts	51

Abstract

A product with good accuracy and strength is always considered as a product of better quality. Accuracy and the strength are always the essential attributes in various RP processes. FDM printing is relatively a typical RP technology which works on the principle of stacking one layer to another to construct a part. In FDM complexity of the part is not a hurdle but there are limitations in every manufacturing process. Accuracy and strength are the attributes which are directly influenced by process parameters. The main initiate of this study is to develop the process planning guidelines to enhance the accuracy of the part fabricated by FDM. Study includes the effect of shrinkage on part manufactured by Reverse Engineering. In Experimentation, shrinkage compensation factor is developed to overcome the shrinkage occurred due to phase change of the material. SCF is been developed on the base of mean method to improve the accuracy of the part. Design of process planning for enhancement of accuracy of the part is also been studied through various experiments. Guidelines were established and confirmed by fabricating parts consisting shrinkage compensation factor. The expected quality of the parts fabricated are counted for each guideline. The outcome of the present research would be fruitful for both the process planner and product designer to manufacture parts by FDM.

Keywords: Design of Manufacturing, Reverse Engineering, Shrinkage Compensation Factor, Fused Deposition Modeling, Accuracy.

CHAPTER 1: INTRODUCTION

Industries nowadays are focusing specially on key features like cost, time and quality to sustain in market due to effect of competition increasing day by day. To withstand the competition, manufacturers needs to make sure that the product must reach market as soon as possible. As well, Quality cannot be compromised to maintain a credible brand name. Better performing product along with cost effective manufacturing system is the prime desire of the industries these days. Additive Manufacturing(AM) system also known as Rapid Prototyping(RP) is supposed to be the perfect solution for the objectives mentioned above. In Rapid Prototyping part is fabricated by piling one layer on another [1]. Rapid Manufacturing (RM), Layered Manufacturing(LM), and Addictive Manufacturing are also the other names of this technology. In Rapid Prototyping models are being automatically fabricated from a virtual 3D CAD model by depositing one layer over another layer, voiding conventional methods, where material is eliminated by several machining processes to get the finalized product [2]. Since its invention till now, there are plenty of expansions into new martials and applications in Rapid Prototyping. RP mastery techniques have overpassed the basic scope of prototyping, there are various examples where parts fabricated by RP are being used for end-use parts. All this is the result of constant inventions being done in research and technology felid of RP. These potentials proven in dissimilar fields has satisfied into growing the operational materials and the scales of using RP.

1.1 Rapid Prototyping

Rapid Prototyping (RP) is a recent trend of production machines in which physical prototypes are directly made from 3D CAD models. In this process part is created layer by layer addictive process where one layer is loaded on another in vertical direction to form a part. In Computer Numerical Control (CNC) machining part is manufactured by a subtractive manufacturing process where in RP part is being fabricated by additive formation process with the help Computer Aided Design (CAD) data. Time consumption of production in Rapid Prototyping is dependent upon the dimensions and complexity of the part. For better visualization of the product, RP offers visual assistance to workers and clients. Prototypes can also be used for the testing of design aspects, Such as tunnel test. With the help of RP, one is managing to produce models which is also termed as ‘Rapid Tooling’, and RP is capable to make purely functional parts and assemblies which are known as ‘Rapid Manufacturing’. RP is best considered to method to form small batch production and complex parts. Due to cost

and time related factors RP is not appropriate for mass production where CNC machines are more efficient. But RP performs magnificently where the complex part is needed to manufacture.

1.2 Historical Development of Rapid Prototyping

Rapid Prototyping is fairly a modern discovery and its progress is closely linked with the advancement of computers in the industry [1]. The falling cost of computers has fortified the improvement in manufacturing industry and introduced innovative knowhows like Computer Aided Design (CAD), Computer Aided Manufacturing (CAM) and Computer Numeric Control (CNC). The first Rapid Prototyping machine introduced to the market was in the late 1980s. The primary patent for Rapid Prototyping technology (RPT) was filed in May 1980 [3]. It was ill-fated that the full patent specification was sequentially not filed by Dr. Kodama before the one-year time bound afterward the request. The first patent for Stereolithography gadget (SLA) was issued in 1986. This patent belonged to Charles Hull, who designed Stereolithography gadget (SLA) machine in 1983 [4]. He went on to co-found 3D Systems Corporation which is one of the major and most creative organizations in 3D printing planetary now.

Table 1.1: Growth of Rapid Prototyping and Similar Systems

YEAR OF ORIGIN	TECHNOLOGY
1770	MECHANISATION
1946	FIRST COMPUTER INVENTED
1952	FIRST NC MACHINE INVENTED
1960	INVENTION OF COMMERCIAL LASER
1961	FIRST COMMERCIAL ROBOT
1963	FIRST INTERACTIVE GRAPHIC SYSTEM
1988	FIRST RP SYSTEM INTRODUCED TO MARKET

About that point of time lot of research was going on in the field of Additive Manufacturing which ran to many expanded technologies to meet the same end necessity. Carl Deckard in 1987 filed a patent in United States for a Rapid Prototyping process which was grounded on laser is known by Selective Laser Sintering (SLS). This patent was issued in 1989 and SLS was later licensed to DTM Inc, which was far along attained by 3D Systems. One

more alternative Rapid Prototyping process called Fused Deposition Modeling arises in 1989, Scott Crump the originator and co-founder of Stratasys Inc. snaked a patent for Fused Deposition Modeling (FDM).

The patent was allotted to Stratasys in 1992 [5]. Some other Rapid Prototyping technologies were also established about these years, namely Solid Ground Curing (SGC) patented by Itzhak Pomerantz et al. Ballistic Particle Manufacturing (BPM) patented by William Masters, Laminated Object Manufacturing (LOM) patented by Michael Feygin, and ‘Three-dimensional printing’ (3DP) patented by Emanuel Sachs et al. In the early nineties, an growing number of competing companies in the field of RP was detected, but only three of the originals endured till now, Which are 3D Systems, EOS and Stratasys.

1.3 Types of Rapid Prototyping System

Since the exhibition of first commercial system in 1988, many processes have been developed. These commonly used RP processes includes:

- 1) Stereolithography (SL).
- 2) Selective Laser Sintering (SLS).
- 3) Fused Deposition Modeling (FDM).
- 4) Laminated Object Manufacturing (LOM).
- 5) Laser Engineered Net Shaping (LENS).
- 6) 3-Dimesional Printing (3DP).

1) STEREOGRAPHY (SL): This method is utilised to construct a 3D model with photosensitive liquid resin which when bare to UV light forms a solid [6]. Figure 1.1 displays the Stereolithography apparatus which is grounded on essential process known as photo polymerization. Due to the absorption and sprinkling of UV light beam, the response takes place and treats the surface, founding a tough layer. When the layer is cured the bed 4 is dropped equivalent to one-layer thickness by an elevation controller to permit the additional layer of resin to likewise form over it. The preserving is done by UV Helium cadmium or Argon laser [1]. A blade is used to spreads liquid resin on the part as the blade crosses the vat. This decreases the recoating time and surface unevenness. The part produced with the help SL is called green part. The green part is then post-cured in an UV oven after eliminating support constructions.

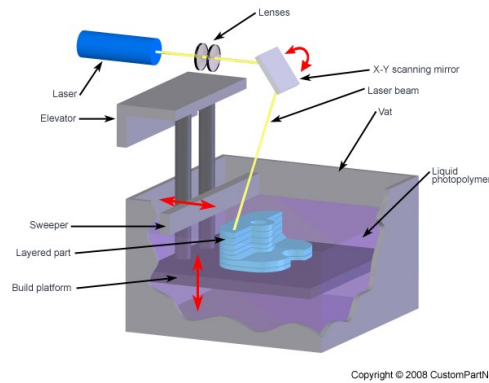


Figure 1.1: Stereolithography [7]

Application Range

- a. Parts made-up by SL are utilized for diverse mechanical tests.
- b. Replicas for medical purpose can be made from SL.
- c. Form-fit jobs for assembly tests.

Advantages

- a. Parts which cannot be fabricated by conventional machining in one go can be fabricated by SL.
- b. No additional supervision is needed which saves time which can be used effectively.
- c. High Tenacity parts can be made through SL system.

Disadvantages

- a. Support structure is essential for SL which rises the material consumption.
- b. Post processing is obligatory in SL system which eventually grows the cost of the part.

2) SELECTIVE LASER SINTERING (SLS): In Selective Laser Sintering process, a high-power laser is utilized to sinter well polymeric material layer by layer. Figure 1.2 displays that the procedure involves with scattering the fine powder (20 to 100 microns in diameter) with the help of rollers [6]. Parts are constructed on platform which is heated up just below the melting temperature of material by infrared warmers to reduce the alteration due to thermal stresses and to sinter the earlier layer with the new-laid layer. CO₂ laser is utilized to scan the deposited layer of powder to sinter the powder particles to produce a solid. The contact of the laser beam with the powder raises the temperature to the point of sintering, melting the powder particles to form a solid mass [7].

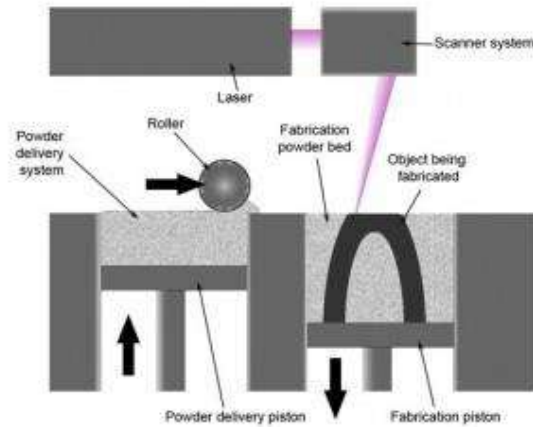


Figure 1.2 Selective Laser Sintering [5]

Application Range

- a. SLS is used for graphic representation of the replicas.
- b. Purposeful parts and intricate prototypes can be fabricated in SLS.
- c. Efficient to cast metallic parts.

Advantages

- a. Different variabilities of material can be utilised in SLS.
- b. Support structures are not compulsory in event of SLS.
- c. Post curing is only mandatory in case of ceramics.

Disadvantages

- a. During solidification, supplementary powder may be hardened at the border line.
- b. The roughness is most visible through the naked eye when parts contain sloping (curved) surfaces.

- 3) **LAMINATED OBJECT MANUFACTURING (LOM):** In the LOM procedure, the solid material in the form of sheet is followed to substrate with a hot roller. Figure 1.4 demonstrate the arrangement which engages a 25 or 50-watt CO₂ laser to split the material. Every layer is cut with the help of a laser, which is curbed to breach to the exact depth of one-layer thickness. Unsolicited material is pared into rectangles to felicitate its exclusion later. But it remains during the build process to help as support structure. The platform with accomplished layer transfers down and a new layer of material is trolled into the position. The process is recurring till the part is fabricated [8].

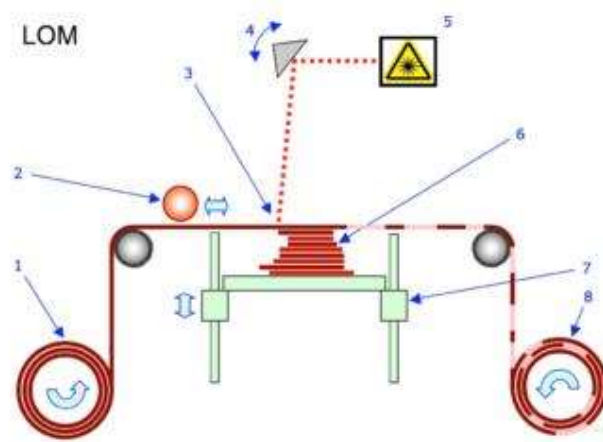


Figure 1.3: Laminated Object Manufacturing [W1]

Application Range

- a. Beneficial for representation of visual models.
- b. Large bulky models can be built by this process.

Advantages

- a. Various forms of organic and inorganic materials can be utilized like as paper, plastic, ceramic, composite etc.
- b. LOM is a faster process than other RP processes.
- c. Due to absence of internal stress generation at the time of manufacturing there is no undesirable deformation.
- d. LOM is capable to overcome discontinuities at the projects, where objects are not closed totally.

Disadvantages

- a. The constancy of the model is exposed to the strength of the layers pasted with one another.
- b. It is difficult to manufacture parts with thin walls towards the direction of build with LOM process, and LOM is not appropriate process for manufacturing hollow parts.

4) LASER ENGINEERED NET SHAPING (LENS): Laser Engineered NET Shaping, also termed as Laser Powder Forming is a rapid prototype technology established for fabricating metal parts. In this method a float substrate made from the metal to be deposited is consumed as a base for part to be manufactured as demonstrated in figure 1.5[9]. To create a molten puddle on the surface a high powered YAG laser in which power is ranging from 250W to 1000W is focused on powder.

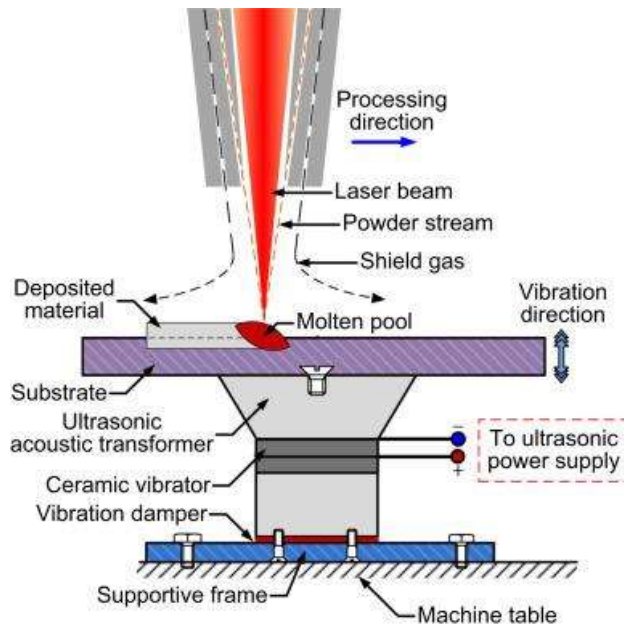


Figure 1.4: Laser Engineering Net Shaping [10]

5) 3D PRINTING (3DP): 3D printing technique consumes a constant filament of thermoplastic material. Figure 1.6 displays that the filament is sucked by a large coil called spool. The material ejects through a heated printer extruder head. After heated up molten material is ejected through the tip of the nozzle. In 3D printer nozzle diameter can vary in size. Solid layers are produced by subsequent a rasterizing motion where the roads are placed side by side within a pervasive domain boundary.

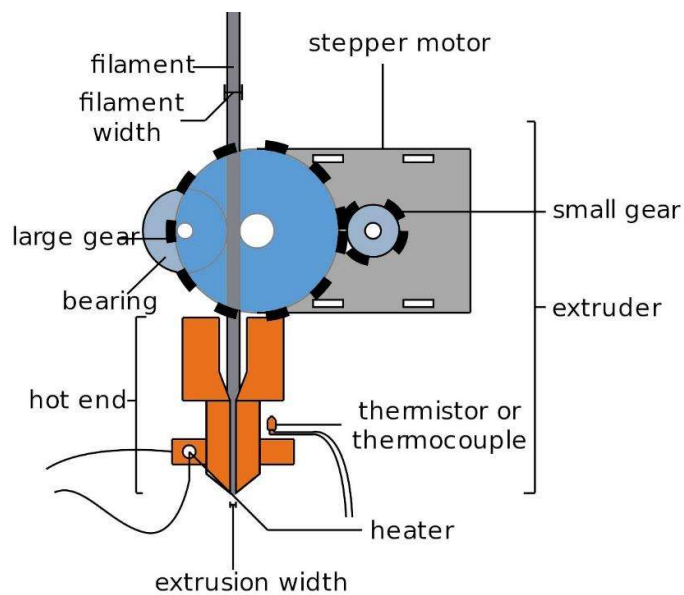


Figure 1.5: 3D Printing [W2]

6) FUSED DEPOSITION MODELING (FDM): In FDM, Material which comes in the form of thermoplastic filament is being heated and extruded by the nozzle. Movement of nozzle tip is in the X-Y direction. Figure 1.3 displays the extrusion head which extrudes very tinny layer of material termed as ‘road’ onto the build platform, which solidifies after falling off temperature to form the model. To reduce the time of solidification the material is heated up just above the melting temperature by virtue material gets instantly solid.

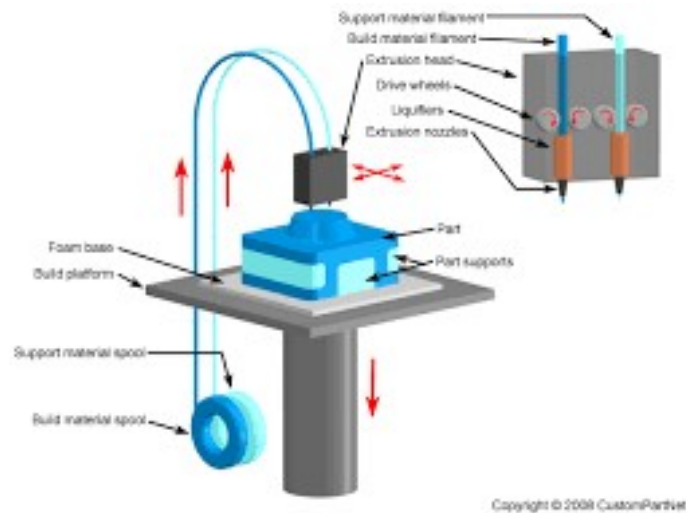


Figure 1.6 Fused Deposition Modeling [13]

Application Range

- a. It is advantageous for Conceptual modeling.
- b. FDM can be rapidly used for Fit and Form applications.
- c. Can be utilised for Investment casting and injection moulding

Advantages

- a. Because manufacturing cost is low, so this process is economical as well.
- b. Elimination of toxic chemicals, liquid chemical bath and lasers make this process informal.

Disadvantages

- a. There is dimensional inaccuracy in parts fabricated by FDM due to phase change in material.

1.4 Process Planning in Rapid Prototyping

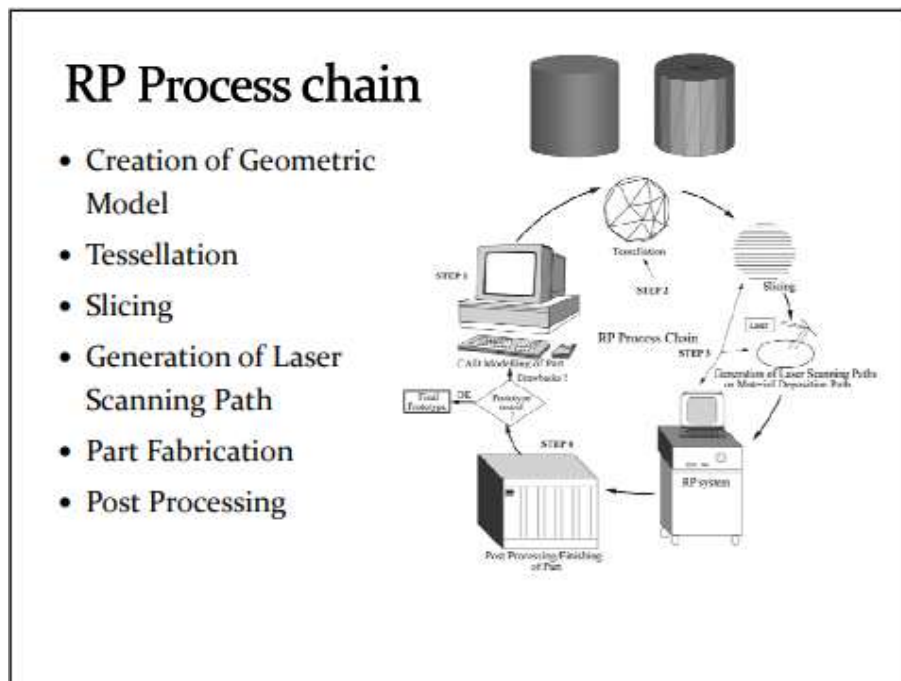


Figure 1.7: Rapid Prototyping Process Chain [1]

Formation of Geometric Model: Rapid prototyping process starts with the creation of a solid model in CAD software.

Tessellation: Tessellation is a process in which the surface of 3D cad model is fragmented by a group of triangles. The tessellated file comprises the information about the group of triangles and the direction of vertices. The quantity of triangles and their size is categorised by facet deviation and chordal height.

Slicing: After tessellation the cad file is sliced with the help of software. RP systems have different slicing software which makes data in standard formats like SLC (Stereolithography contour), CLI (common layer interface) or .X3G etc.

Process Parameters: Process parameters varies along with different process software. Various process parameter software can control Layer thickness, raster angle, infill, bed temperature, extruder temperature etc.

Part Fabrication: After deciding process parameters the software generates a G-code file which is legible by the machine, different machine recites different formats of file. This file is suckled to the machine with the help of card reader or pen drive and the part fabrication initiates.

Post Processing: RP is a layered manufacturing process, where stair casing and support structures can result surface roughness. Therefore, post processing is obligatory in some cases. Sanding, polishing, painting and chemical brushing are some type of the processes used for refining surface finish.

1.5 Problem Areas in Rapid Prototyping

During the recent trends manufacturing sector is needing constituents like limitation of product development cycle, products to match international standards, to decrease the huge investment risk of advancement of new products and to increase to profits. These factors are the primary keys of survival nowadays. Rapid prototyping is developing in such manners to meet these requirements. Still there are various issues which are in relation with the research in RP. Some of the problems faced in RP is discussed below:

- 1) Accuracy of the Part:** Various parts in RP systems are fabricated with the help of Thermal Processes due to which the problem of distortion of part arises. That distortion is known as curling. Mercelis and Kruth[10] defined this curling as the lift of the lowest edge of the part. Various process parameters like humidity, temperature etc are main cause after the deformation of the part. Figure shows the effect of curling in the part.



Figure 1.8: Curling of Parts [10]

- 2) Strength of the Part:** Parts fabricated by RP technologies are cannot be compared with the parts manufactured by conventional machining in terms of strength. However, RP systems are capable to fabricate the metallic parts as well. In plastics strength of the parts be contingent on numerous factors like orientation, infill percentage and temperature of bed and extruder, pattern of infill etc.
- 3) Roughness of Surface:** Due to layer by layer deposition process of RP, stair stepping formation effects the surface of the part built. Roughness on the surface is formed towards the direction of built. In figure 1.9 one can easily assume the effect of stair stepping formation.

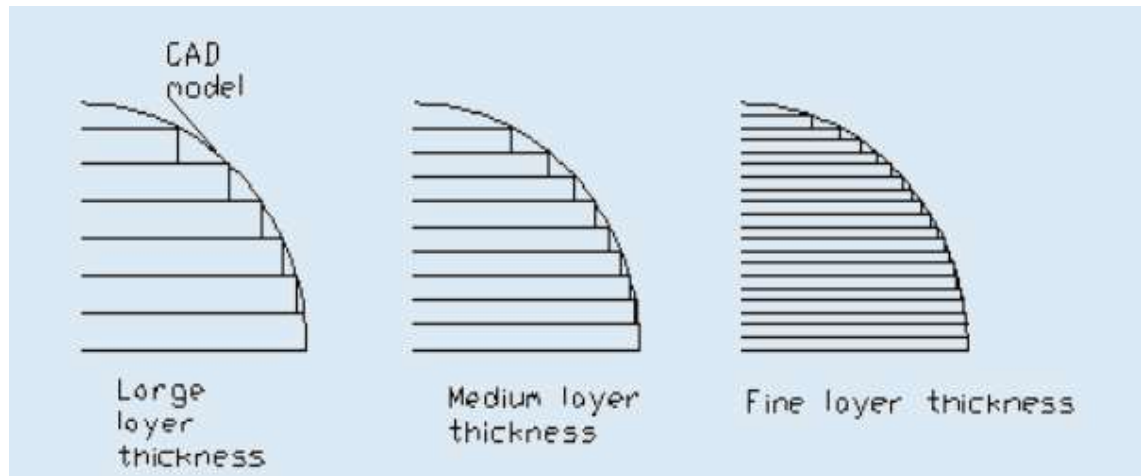


Figure 1.9: Stair Stepping

- 4) Shrinkage in Part Fabricated:** In RP processes one of the major issues is the dimensional accuracy of parts fabricated. Phase change of material causes the shrinkage which results into dimensional shape aberrations. At the time of crystallization, the molecules of the part lodge less volume and then leads to form material shrinkage. In the end, to meet industrial requirements parts fabricated by RP must have good strength and dimensional accuracy. In the next chapter there will be discussion about the research literature in relative areas of development in the field of RP and major reforms pursued to enhance the strength and accuracy of part.

CHAPTER 2: Literature Review

Since the introduction of Rapid Prototyping, various researches are going on to enhance the layered manufacturing techniques. However, the fundamental process of rapid prototyping remains the same i.e. layer by layer manufacturing. The input variables for all techniques change accordingly. Process parameters in rapid prototyping directly influence the dimensional accuracy, strength and surface finish of respective parts.

It is important to evaluate the existing research and development going on in the field of rapid prototyping. Further, it is significant to analyse different process parameters for the refinement of strength, accuracy, and surface finish of the part. The rapid prototype parts are formed by additive manufacturing process, where the properties of each part are comparatively different from the parts produced by conventional manufacturing processes. Although, a direct comparison is difficult [7].

In FDM printing of the objects, shrinkage can become a major issue. The most commonly used types of plastic for conventional FDM printing is ABS (Acrylonitrile Butadiene Styrene). Intrinsically, ABS is stronger and more flexible, but is non-biodegradable. When ABS get cool after printing it shrinks approximately about 8%, although this will vary somewhat depending on the material used. In context to rapid prototyping, many researchers have worked to improve the manufacturability of the components using different rapid prototyping technologies [11].

Majority of the existing research efforts in the DFM for rapid prototyping parts is limited to the shrinkage of parts in longitudinal direction only, however, there hasn't been a concrete research on the influence of shrinkage on free form surfaces created by the additive manufacturing process, which has been explored in this research paper.

2.1 Risk Factors/Uncertainties/Possible Sources of Error

With the changing paradigms of the manufacturing sector, the product development cycle has considerably reduced. This has been aimed to minimize the investment risk involved in the development and production of new products [12]. Considering the changing aspects of the manufacturing sector, rapid prototyping has some pitfalls, which require an important resolution. These challenges are:

- a. **Part Accuracy:** Majority of the RP processes are thermal in nature and hence, there is a common problem with all the RP related processes, called as curling. Intrinsically, it is the distortion of the certain part that is linked with the distortion

of bottom edges of the part. The deformation can occur due to different factors such as: temperature, material used, humidity, and process parameters.

- b. **Shrinkage:** Another issue related to the rapid prototyping processes is the dimensional inaccuracy. Certain parts are subject to shrinkage due to material phase change, which can cause dimensional inaccuracy. In addition, during the process of crystallization, different molecules are arranged randomly and may occupy less volume that can cause shrinkage [13]. Specifically, in the case of free form surfaces, shrinkage occurs due to the lack of uniformity in the shape of the different parts.

2.2 Studies related to the Accuracy and Strength of the Part

Torrado et. al [13] discovered that to create materials with amplified physical properties, an addition of reinforcing materials can be an instrumental approach. Surface finish was refined with augmentation of an elastic material with ABS and the effect of the experiment was clearly visible as we compare the ABS baseline material. Although, there are some drawbacks of this inclusion, as well. Extrusion temperature of this material was comparatively high, over 300 C. Influence of the inclusion was also prominent on the mechanical properties and fracture surface, as we compare it to pure ABS.

Baich And Manograham [14] explored that print parameters such as: infill patterns impact the mechanical strength and print cost. Their research exhibited the connection between mechanical properties and infill pattern selection, along with production time and the final part cost. In conclusion, low density parts can be used in tensile applications. These efforts can save money as well and strength of the product is not affected.

Hernandez et. al [15] defined that build angles can affect the mechanical properties of the parts in 3D printing. In the experiment, 45 different samples were constructed in 5 distinct orientations; 0 degrees in the XY plane, 45 degrees in the XY plane, 90 degrees in the XY plane, 45 degrees in the Z plane, and 90 degrees in the Z plane. It was revealed by the outcome that highest tensile strength was obtained by printing 90 degrees in the XY plane. Parts built at 0 degree on the XY plane had extra compressive and flexure strength comparatively than parts built with other orientations. Build orientation is a disfiguring factor for the strength, stiffness and toughness of the part, depending upon the application.

Boschetto et. al [16] completed a study on macro and micro geometrical aspects of the RP model by testing prototypes with the help of a profilometer. The main objective of the study was to forecast the dimensional deviations of models produced by FDM. The authors concluded that shape warpage affected surfaces with minute dimensional deviations. The result

of the study showed that the model predicted dimensional deviations and provided information about geometrical tolerance, as well.

Kulkarni and Dutta [17] examined the different deposition techniques in FDM operations. Rather than using conventional methods of deposition path, composite modeling was executed. The research concluded that composite laminated analysis was consistent and helpful while choosing a deposition strategy as according to stiffness requirements. The results showed that the refined deposition techniques were superior than the conventional methods.

Masood and Song [18] developed a unique polymer composite material for the FDM process utilized in the rapid tooling technique. Iron particles in the nylon type matrix was used as the material. After testing it was observed that materials of large filler particles of uniform size manifested lower tensile modulus. On the other hand, composite with tiny particles showed tensile elongation.

Kwan [19] proposed the fabrication of rapid prototype parts directly from the data obtained by reverse engineering. A specific algorithm was developed to reduce the size of point cloud data. Further, the surface data was extracted by laser scanning technique. The method was implemented on two different parts. It revealed that better accuracy was achieved by using reduced point data models.

Paulic et. al [20] produced a part contacting free formed surfaces with the help of 3D scanning technology and obtained point cloud data of an existing object. A CAD model was developed for a button pair which had been used in automobiles. The study revealed that the combination of rapid prototype and reverse engineering can be instrumental in producing already existing projects.

Yaodong et. al [21] considered the impact of material shrinkage affecting the accuracy of parts produced by rapid prototyping. With the help of data analysis, the research introduced a law of shrinkage for the deformation of prototypes. A recreation equation was applied to the dimensions of a part in manufacturing to meet the accuracy required for assembling the parts. Material shrinkage rate and material filling rate, which is necessary for the reference of model scaling was obtained through experimental formula

Firstly Tian-Ming et. al [22] developed the mathematical model to refine the wrap deformation. The research revealed major influencing factors of deformation. The features affecting the procedure were material characteristics, setup of fabrication parameters and geometrical structure of CAD model. Based on the conclusion of the model analysis, the research explained different pitfalls, issues and related phenomena in the FDM process.

You-Min and LAN [23] disclosed the effect of path planning for obtaining accuracy in stereolithography. To achieve dimensional accuracy and decrease the curls distortion, a simple, effective and proper laser scan path planning was purposed. A connection between the geometric profile and different scan path were exhibited in the research. By the compensation of profile scanning, a CAE simulation code was developed to support the RP fabrication. K Senthilkumaran et al. [24] introduced an advanced shrinkage compensation method by reimbursing the geometry along the single direction Drexel Space, to handle non-uniform shrinkage. A software was developed to attain the compensation of STL and a layered file.

In the research presented by Schmutzlera et al. [25], the author has elaborated the implementation of free form deformation to adjust the prominent appearing defects in the process of 3D printing. Further, the research also proposed a unique methodology for handling the distortion in the STL data. The proposed technique was a novel method to recreate and compensate any distortion commonly occurring in the process. In addition, with the pre-deforming of the construction data, enhancement in the size accuracy can be achieved.

Dao [26] introduced a new compensation factor for the products produced in Stratasys machine. For producing parts on by ABS the shrinkage compensation factor of 1.010 was helpful to reduce 53% in mean error. Pandey et al. [27] studied the important effects of orientation in fused deposition modeling. The authors introduced a tool which recommended the most efficient orientation for different parts according to the requirement. In addition, genetic algorithm optimisation technique was used to define the ideal part orientation.

Nosouhi and Rahmati [28] examined original technique to feign the shrinkage in stereolithography parts. It has been originating that shrinkage typically happens while stake curing in UV chamber. The FE simulations were completed as the curing curves produced by laser movement on resin surface. Precisely, STAR-WEAVE hatching technique was replicated. The consequences evidently presented that the shrinkage was condensed remarkably consuming this new hatching method.

Williams and Deckard [29] deliberate the systematic delinquent relating the energy delivery, heat transfer and sintering procedure with additional relevant phenomena. Physical trials and application of a numerical simulation were showed consuming Bisphenol polycarbonate. The consequences of nominated strictures like laser power, hatch spacing, and scan line length on the SLS process have been inspected. It was originating that subordinate procedure constraints like delay period have a important impact on the process response.

Gregorian et al. [30] explored the in-plane accurateness of FDM-1650 machine and presented the result of best Shrinkage Compensation Factors (SCF) on the correctness of the

parts. The data was analysed for correctness using average formulations and figures, such as standard deviation, rms error, etc. The optimum SCF for the FDM-1650 machine was originating to be 1.007 or 0.7%

2.3 Gap in Literature

By reviewing the literature, it is observed that the research work still obtains some gaps and this research can contribute to eliminate the loopholes.

1. As FDM printing is not a new concept, however there is no work done on the shrinkage of free form surfaces.
2. The fabrication of Rapid Prototyping part depends upon the ascertain value of process parameters and machine parameters which is very difficult to discover without performing some experimentation.
3. It is very difficult to predict the shrinkage and curling of RP parts because these defects generally tend to be non-symmetrical.

2.4 Research Objectives

Objective of this research work are detailed below:

- a) To study the effects of shrinkage on the free form surfaces of the FDM printed parts.
- b) To study the effect of process parameters on the accuracy of the part using Reverse Engineering and Coordinate Measuring Machine.
- c) To determine the shrinkage compensation factor for different type of surfaces.

2.5 Methodology

The objective of this work is to provide the compensation factor for surfaces to enhance the accuracy of the FDM printed parts. To achieve these, following steps are taken into consideration:

- Select four different surfaces based on the literature survey.
- Fabrication of parts containing these surfaces with the help of CNC machine.
- Measuring dimensions of parts manufactured on CNC machine by CMM.
- Development of CAD model with the dimensions measured by CMM on CNC manufactured parts.
- Printing of the CAD model using FDM machine.
- Measurement of printed parts by using CMM.
- Shrinkage calculation of FDM printed parts against the dimensions measured from CNC fabricated model.
- Redefining the CAD model and printing of part including compensation factor.

- Reverse engineering of CNC developed part to generate CAD model.
- Interference analysis of reverse engineered CAD with CAD model containing shrinkage compensation factor to determine any surface inaccuracy.
- If any interference is found, provide suitable compensation in the CAD model containing shrinkage compensation and then regenerate the CAD model which will contain shrinkage as well as interference tolerances.

CHAPTER 3: Planning of Experiment

By reviewing the literature, it has been concluded that many researchers have worked to enhance the quality of parts manufactured with RP techniques by implementing various parameters. RP is a new technique, so there is lack of process planning guidelines for improving the accuracy of parts. Problems are faced when it comes to the printing of parts having some typical surfaces. The main purpose of the research is to enhance the accuracy of parts having surfaces which are not traditional. For pursuing the research, there is need to identify the input variables which directly effects the shape of the parts manufactured. With this adjustment the accuracy of the parts produced can be maximised.

Accuracy and strength are the attributes which are directly influenced by process parameters. The main initiate of this study is to develop the process planning guidelines to enhance the accuracy of the part fabricated by FDM. All the details of Fused Deposition Modeling are discussed in section 3.1.

3.1 FDM Process

Fused Deposition Modeling (FDM) process fabricates 3D objects with the help of 3D CAD data. Thermoplastic material is extruded layer by layer by a temperature-controlled head. The FDM process flinches with an STL file of a model into a pre-processing software. This model is oriented as according to requirement of the shape of the part and carved into horizontal layers variable from +/- 0.127 – 0.254 mm thickness.

A support structure is created needed, based on the position and geometry of the part. After that toolpath is generated. The arrangement functions in X, Y and Z axes, fabricating the model by one layer at a time. The process is same as to how a hot glue gun extrudes melted beads of glue. Thermoplastic material is heated and suckled into the temperature-controlled extrusion head. The head extrudes and leads the material with accuracy. The outcome of the tough material covering to the preceding layer is a plastic 3D model built up. After finishing the part supports are removed and finishing of surface is done.

Figure 3.1 shows the FDM printing machine uPrint SE from Stratasys having built volume (8" × 6" × 6"). It uses ABS M30 material and SR-30 as a supportive material which is a soluble support. It is available with a software called 'Catalyst EX' which helps to attain required parameters which are important for fabrication of the part.



Figure 3.1: Stratasys uPrint SE

Various process parameters of FDM is listed below-

Height of Layer: In maximum of the Rapid Prototyping procedure the fabrication takes place by fabricating one layer on another in z-direction to attain part. Layer thickness is the parameter which can directly influence the surface roughness and part build time. Layer thickness of the part to be manufactured can vary from 100 microns to 400 microns. Surface roughness will increase with increasing the layer thickness and there will be reduction in the build time.

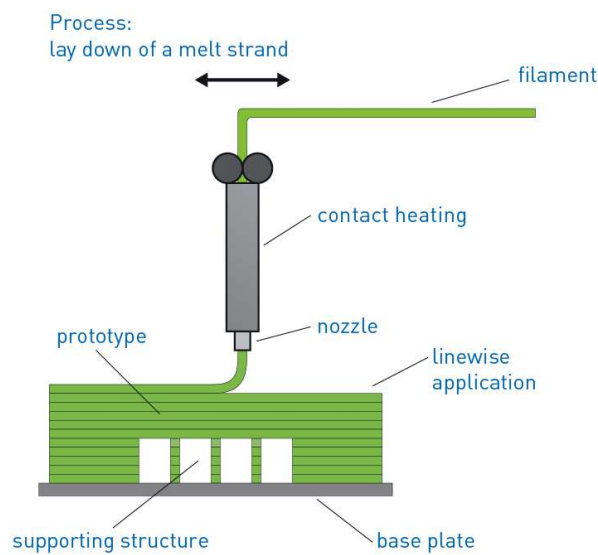


Figure 3.2: Layer by layer deposition in Z direction [W3]

Temperature of Extruder: In various FDM machines extruder temperature can be set through the software. Extruder temperature may vary as according to the material used for printing. Different material has diverse extruder temperature.



Figure 3.3: Extruders of FDM Machine

Part Bed Temperature: Part bed temperature is the temperature of the build platform. It diverges from material to material and depends upon the glass transition temperature of the material.



Figure 3.4: Build Platform

Infill Pattern: The software ‘Catalyst EX 4.5’ provide different infill pattern, these patterns are used to infill the interior of the part being fabricated. The different infill patterns have different style of laying the material. Solid pattern is used where high strength of part is required. Sparse high density is used where moderate strength is needed. Sparse low density is used where part is used for demonstration only.

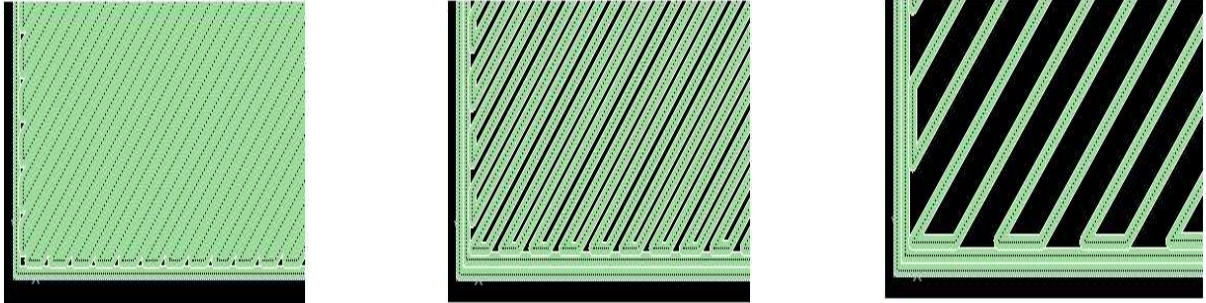
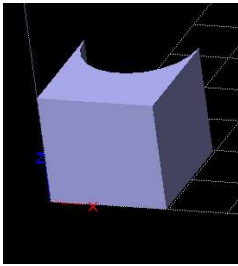


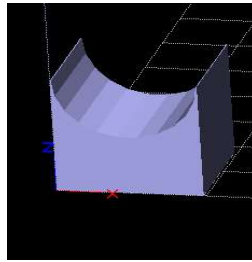
Figure 3.5: Infill Pattern

Printing speed: Printing Speed is the distance traveled per minute by the extruder of FDM machine. Printing speed directly effects the surface finish of the product. The more will be the printing speed the less will be the time to manufacture part.

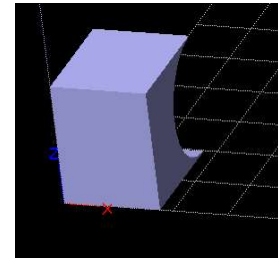
Build Orientation: In Rapid Prototyping, there is lavishness to move or rotate part as according to shape of the part. Part orientation is helpful while saving material. One can orientate part in such a way where support material can be eliminated if possible. Part orientation is one of the important parameters.



a) X-Y Orientation



b) Y-Z Orientation



c) Z-X Orientation

Figure 3.6: Orientation of Part

3.2 Material Properties

Acrylonitrile butadiene styrene (ABS) is a frequently used thermoplastic material for Fused Deposition Modeling. The material in our research is advanced form of ABS. ABS-M30 is up to 25 to 70 percent tougher than standard ABS and is a perfect material for conceptual modeling, functional prototyping, manufacturing tools and production parts. ABS-M30 has greater tensile, impact and flexural strength than standard ABS. Layer bonding is significantly stronger than that of standard ABS, for a more durable part. Table shows the properties of ABS-M30 Material

Table 3.1: Properties of ABS-M30

Property	Value	Unit
Tensile Strength	31 (XZ) Axis	Mpa
Glass Transition	108	°C
Melt Flow	18-20	g/10 min
Tensile Modulus	2180	Mpa
Density	1.04	g/cc

3.3 Mean Method

Mean Method has been used to obtain the standard deviation and arithmetic mean of the set of a specific data. This is the easiest way to calculate accurate values. This method is quick and handy as well. During working with this method, to obtain an average there is one formula used. There are many ways to manipulate this formula to create different iterations on mean complications.

The following is the formal mathematical formula for the arithmetic mean (a fancy name for the average).

$$A = \frac{1}{n} * \sum_{i=1}^n x_i$$

A = average (or arithmetic mean)

n = the number of terms (e.g., the number of items or numbers being averaged)

x_1 = the value of each individual item in the list of numbers being averaged

The following is the formula for the arithmetic mean, stated in a more readable and understandable form.

$$A = \frac{S}{N}$$

A = average (or arithmetic mean)

N = The number of terms (e.g., the number of items or numbers being averaged)

S = The sum of the numbers in the set of interest (e.g., the sum of the numbers being averaged).

3.4 CMM

CMM is a measuring device which detects the surface of object with the help of a contact probe. The probe moves in 3 axes to attain the X, Y and Z co-ordinates of the point. The part to be measured is placed on the measuring table. The points obtained from the surface of the object are transferred into a geometry data file. A CAD model can also be generated with the help of that file. The main outcome of the process is that the shape of the object is captured in form of a CAD file and can be modified as according to need.

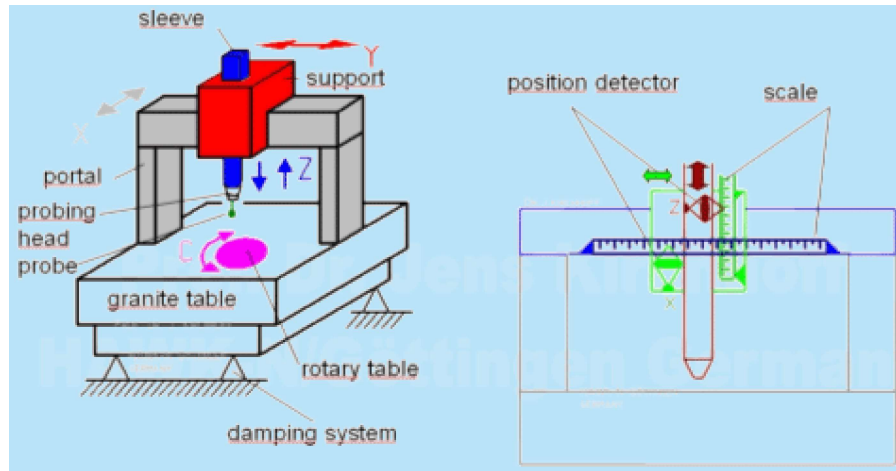
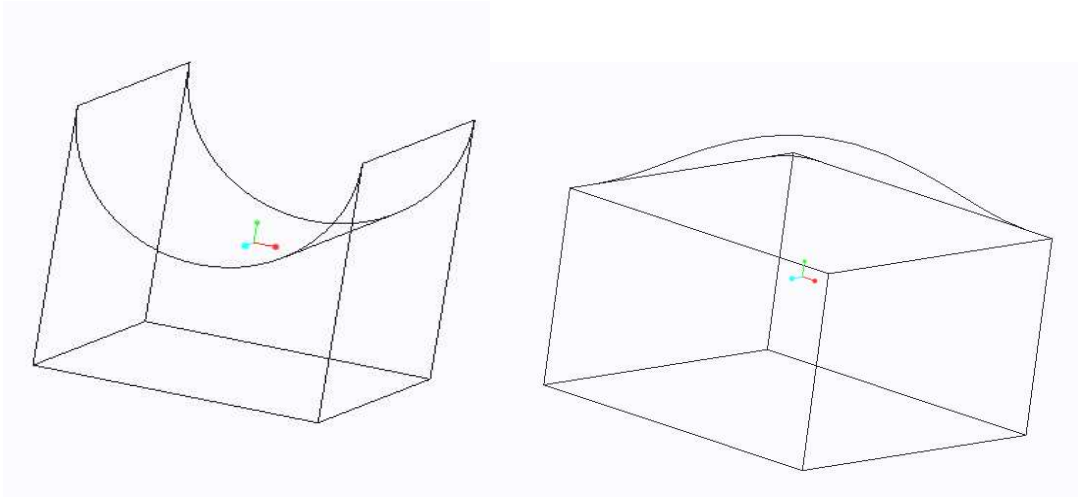


Figure 3.7: Co-ordinate Measuring Machine [W4]

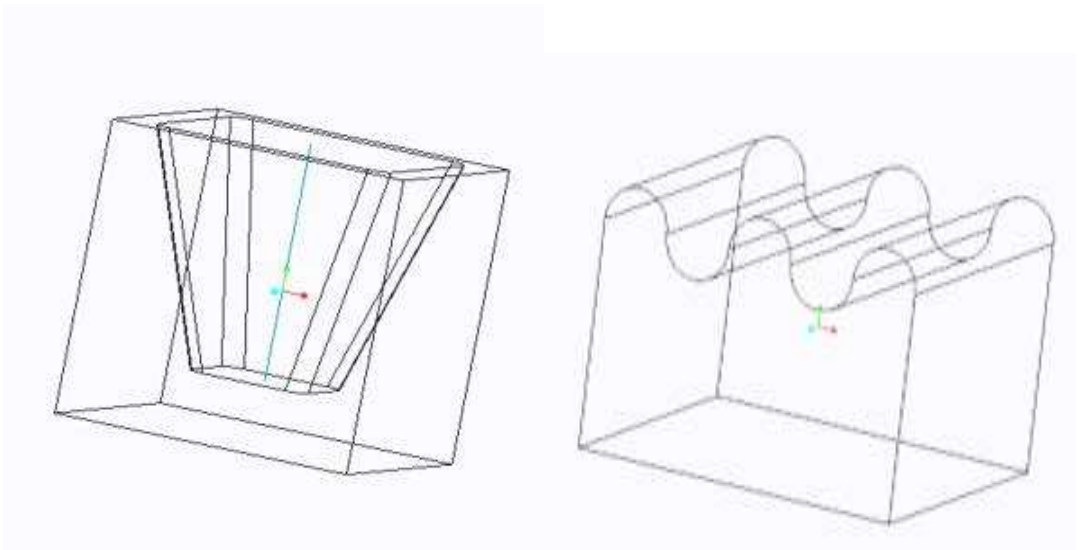
3.5 Selection of Typical Surfaces

The most important aspect of the experiment was the selection of the surfaces. The selection of surfaces has been completed on the behalf of the applications. The surfaces with the large number of applications have been selected. The prime focus of the research was to examine the causes which are directly influencing the accuracy and the shape of the part. As we know there are large number of utilities of RP in the medical field as well. So, the surface selected must have included some features which will be fruitful in that felid also. The surfaces which are decided on the behalf of the literature review are shown in the figure 3.8. For the easiness in understanding the four different parts are classified into four parts that is A, B, C and D. This naming will continue for the whole research.



A

B



C

D

Figure 3.8: Four Selected Surfaces

3.6 Fabrication of Surfaces

The models have been built with the Aluminium using ACE MCV-450. Ace MCV-450 is a 3-Axis vertical milling centre which is utilized for building the four models. Various details of VMC are discussed in the table.

Table 3.2: Specification of VMC

Description	Units	Value
Table longitudinal travel (X-Axis)	mm	800
Table longitudinal travel (Y-Axis)	mm	450
Table longitudinal travel (Z-Axis)	mm	500
Table Size	mm x mm	1000 x 450
Max. load on table	kg	700
Spindle speed	rpm	8000
Spindle power	Kw	11

Based on the design of the experiment, models with variance in shape have been fabricated. Total number of four number of models have been manufactured. Figure 3.9 demonstrates the manufacturing of part with the help of VMC.



Figure 3.9: Fabrication of Parts

All the components have been established by the same machine. The dimensions of the components have been considered in millimetre. The details pictures of the parts are demonstrated in figure 3.10. The programming code of these parts is attached in Annexure 1.



Figure 3.10: Parts Fabricated by VMC

3.7 Measurement of Aluminium Models

After the fabrication of the parts with the help of VMC the next step was to measure these models. Spectra Co-ordinate Measuring machine has been used while measuring these parts. This machine is high end equipment which is used for high precision measurements. Picture of Spectra CMM is shown in the Figure 3.11.



Figure 3.11: Spectra CMM

Measurement of all the four aluminium models have been completed easily with the utilization of CMM. Part A, B, C, and D have been investigated simultaneously. The details of the measured parts are briefed below. A copy of the measurement obtained by CMM is attached on the Annexure-2.

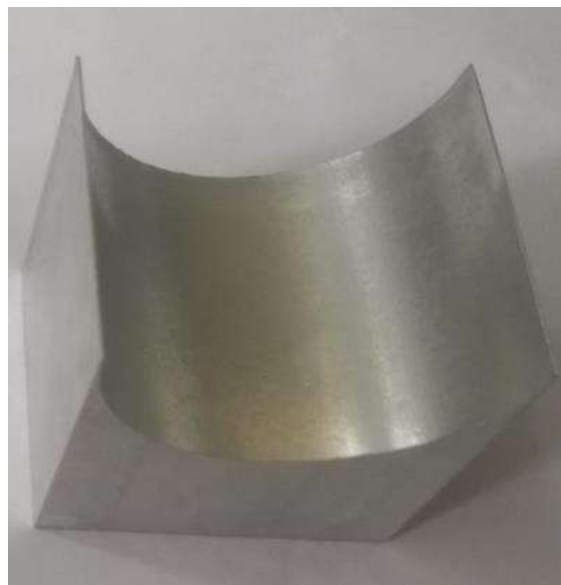


Figure 3.12: Part (A)

Table 3.3: Dimensions of Part (A)

Length	49.89 mm
Breadth	44.66 mm
Height	49.63 mm
Diameter	49.19 mm

Figure 3.13: Part (B)



Table 3.4 Dimensions of Part (B)

Length	53.31 mm
Breadth	50.40 mm
Height	50.32 mm



Figure 3.14: Part ©

Table 3:5: Dimensions of Part ©

Length	52.97 mm
Breadth	50.57 mm
Height	50.84 mm
Inner Length	39.22 mm
Inner Breadth	39.70 mm



Figure 3.15: Part (D)

Table 3.6: Dimensions of Part (D)

Length	49.95 mm
Breadth	44.27 mm
Height	34.86 mm
Upper Diameter 1	9.94 mm
Lower Diameter 1	9.88 mm
Upper Diameter 2	9.95 mm
Lower Diameter 2	10.00 mm
Upper Diameter 3	9.94m

3.8 CAD Modeling

After completion of the measurements by Co-ordinate Measuring Machine the next step was to make a CAD model for all the four parts. For generation of CAD model PTC Creo Parametric 3.0 has been used. PTC Creo Parametric 3.0 is a high-end modeling software which is used widely throughout the industry. The software is equipped with number of commands which helps the user to attain the design required as according to the user. The interface of the software is very user friendly and software is updated frequently. With the help of dimensions

measured by CMM, CAD model of all the four parts generated. In figure 3.16, there all the details of CAD models generated along with the dimensions.

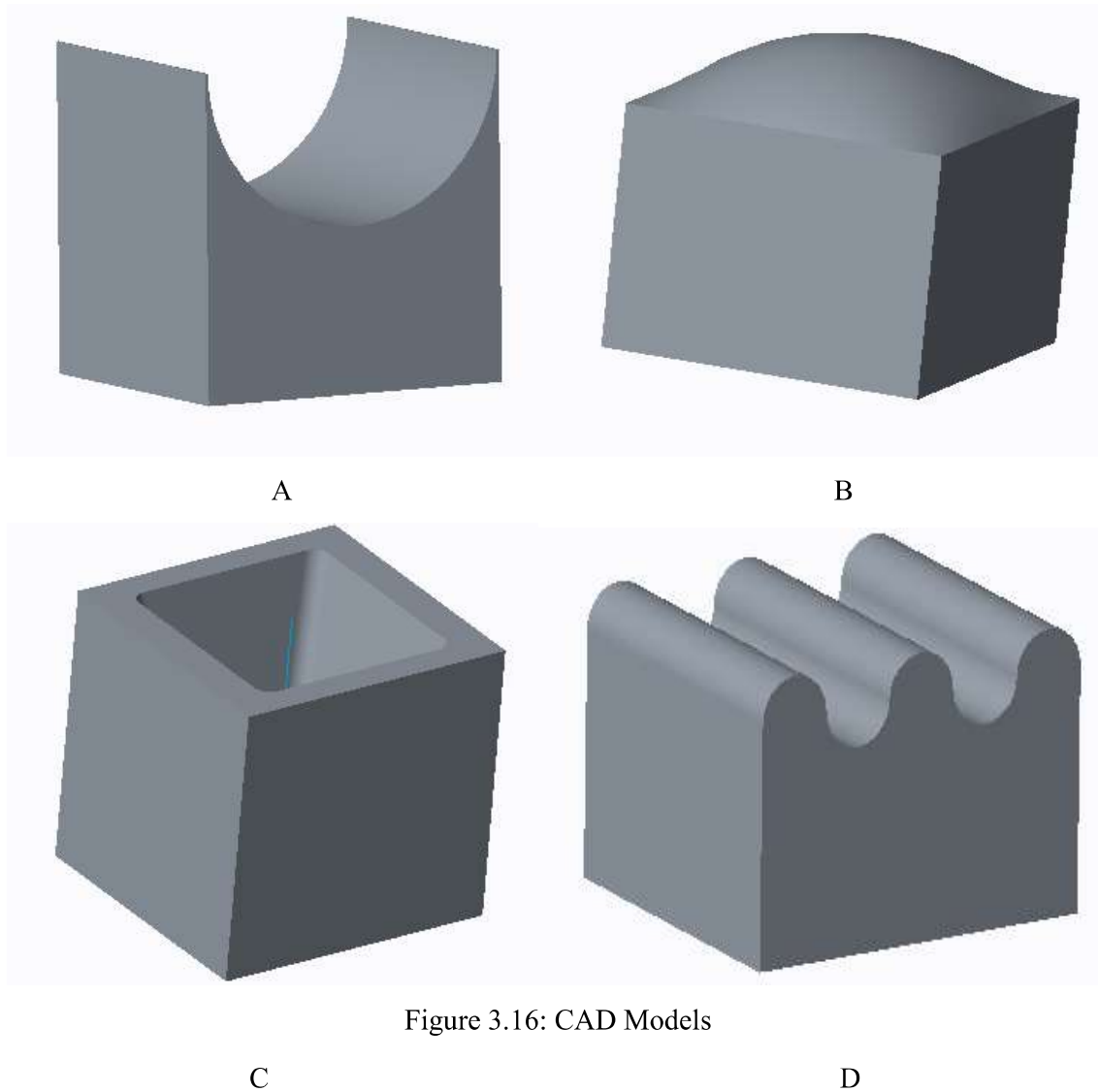


Figure 3.16: CAD Models

Format of the file generated by PTC Creo Parametric 3.0 is the .prt format. But software also provides legacy to convert the file generated into the various formats. The universal format used for fabricating RP parts is stereolithography (.stl) format. In PTC Creo Parametric 3.0, File can be easily converted from .prt format to stereolithography (.stl) format.

3.9 Part Fabrication in FDM

The specimen has been built with the ABS (Acrylonitrile Butadiene Styrene) material using Stratasys uPrint SE. The Cad model has been created according to the ASTM D-638 standard. Various parameters have been selected during the fabrication of parts in FDM. Layer resolution of 0.0100 has been used. High density model interior and smart option of support

fill has chosen to avoid any wastage of the material. In the figure, various parameters and, the orientation of the model is demonstrated.

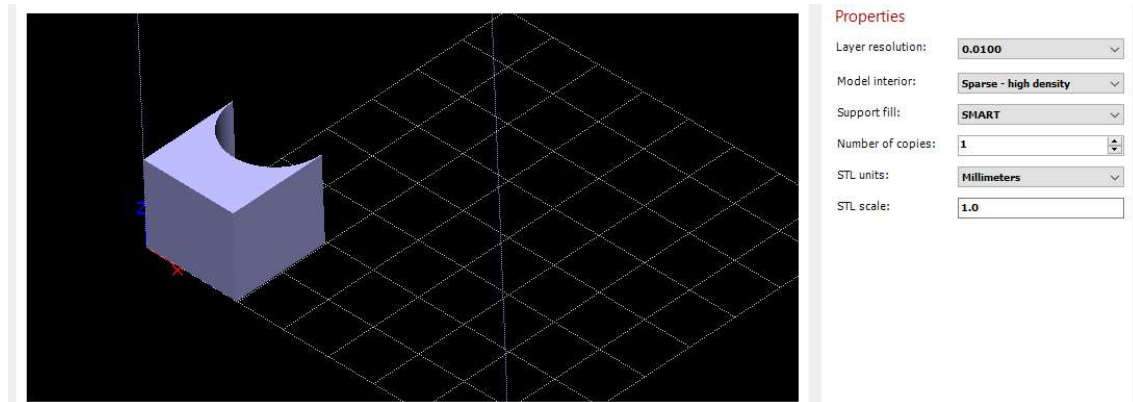


Figure 3.17: Process Parameters in FDM

Post processing treatment has been applied to all the specimens for the finishing. Support structure used in Stratasys uPrint SE is completely soluble. To finalize the product, part prepared by FDM is drowned in liquid which eliminates the soluble support of the structure. In Fig 3.18, parts are illustrated which are fabricated by the FDM.

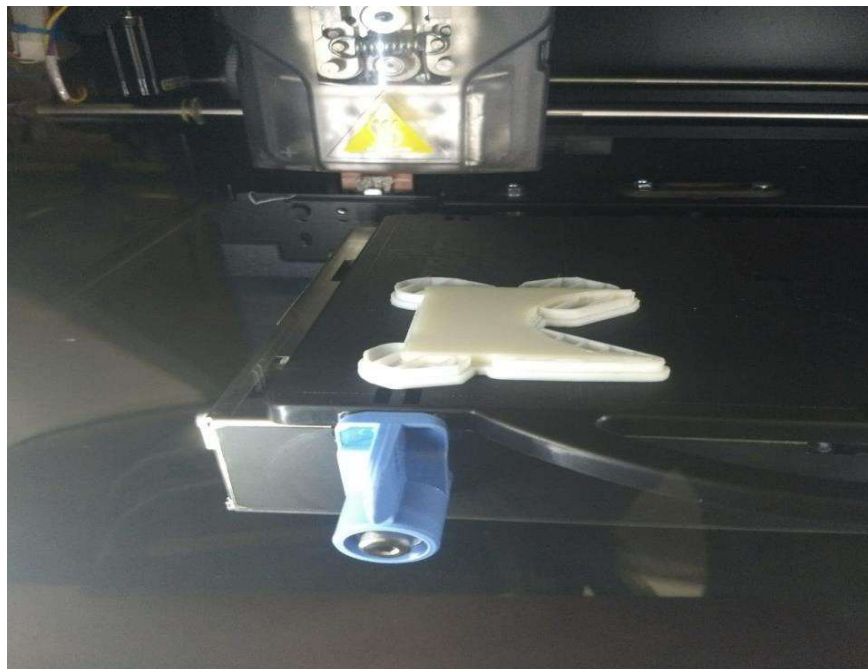


Figure 3.18: Part Produced by FDM

3.10 Study of Shrinkage

Shrinkage is a normal phenomenon in many rapid prototyping processes due to the phase change of the material. In fused deposition modeling, material comes in the solid form which is in the shape of a wire. During the processing material is heated up and it changes its

phase from solid to liquid so that it could flow and form a layer. In the end, material gets solidify which is also a phase change. Due to this change of phase the finalize product suffers with some shrinkage. This shrinkage directly influences the dimensional accuracy of the part. The next step of the research was to identify dimensional errors occurred due to shrinkage. To find the error, parts produced by fused deposition modeling have been inspected by co-ordinate measuring machine. There may be variations of dimensions at different points in ABS part due to effect of shrinkage. While taking dimensions each segment of the part has been fragmented into 10 equal points and highlighted them with the help of marker to get precise dimensions. Finally, mean of all these ten dimensions has been concluded as the main dimension. The measurements taken by co-ordinate measuring machine are described below.



Figure 3.19: ABS Part (A)

Table 3.7: Dimensions of ABS Part (A)

Length	49.76 mm
Breadth	44.60 mm
Height	49.26 mm
Diameter	48.59 mm



Figure 3.20: ABS Part (B)

Table 3.8: Dimensions of ABS Part (B)

Length	53.06 mm
Breadth	50.07 mm
Height	49.9 mm



Figure 3.21: ABS Part (C)

Table 3.9: Dimensions of ABS Part (C)

Length	52.75 mm
Breadth	50.34 mm
Height	50.46 mm
Inner Length	39.30 mm
Inner Breadth	39.75 mm



Figure 3.22: ABS Part (D)

Table 3.10: Dimensions of ABS Part (D)

Length	49.55 mm
Breadth	44.20 mm
Height	34.70 mm
Upper Diameter 1	9.89 mm
Lower Diameter 1	9.91 mm
Upper Diameter 2	9.93 mm
Lower Diameter 2	10.02 mm
Upper Diameter 3	9.87 mm

Chapter 4: Reverse Engineering

In profession of engineering, various branches like manufacturing, designing, maintaining products, structures and systems are involved. Forward Engineering and Reverse Engineering are two groups in which whole engineering could be classified.

Forward engineering is the procedure of conversion of calculated concepts and designs to the physical application of a system.



Figure 4.1: Forward Engineering

Reverse Engineering is a process in which a replica of a product is being created without any help of drawing, computer model, or documents.

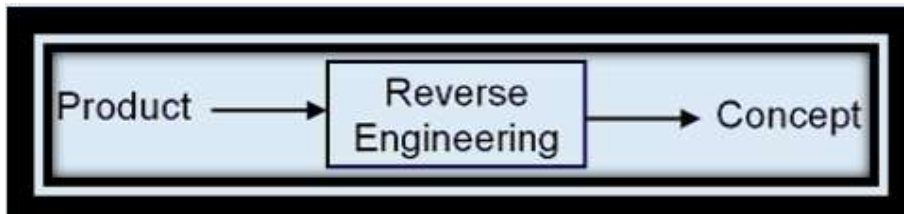


Figure 4.2: Reverse Engineering

Reverse engineering comprises the procedure of exploring a prearrangement to know its mechanisms and their connection, to establish illustrations of it in additional form or a progressive idea. A noteworthy purpose for application of reverse engineering have reduced the expansion time of product. In the strongly competitive global market, producers are continually looking for new ways to abridge lead-times to make a new product. For example, there is requirement to reduce the time of developing tool and die in the field of injection moulding industries. With the help of reverse engineering, a 3-D model can be quickly captured and exported for Rapid Prototyping or manufacturing.

Important reasons behind the implementation of Reverse Engineering

- Production of original product is being stopped.
- Documentations of original design is not available.
- When products are still in demand, but manufacturer no longer exists.
- For the improvement of some bad features in the design of the product.
- Reinforcement of good working product so that the product could be used in long term.
- To relate the features of creation formed by participants.
- To discover new techniques to expand product performance.
- The unique CAD model is not adequate to provision changes.
- To apprise outdated ingredients or old-fashioned manufacturing processes with less-expensive technologies

Reverse engineering starts with the creation and works through the design process in the conflicting way to attain a product description report. To achieve so, it exposes as much data as conceivable about the design ideas that were castoff to produce a product.

4.1 Methodology

The main steps of reverse engineering are discussed below:

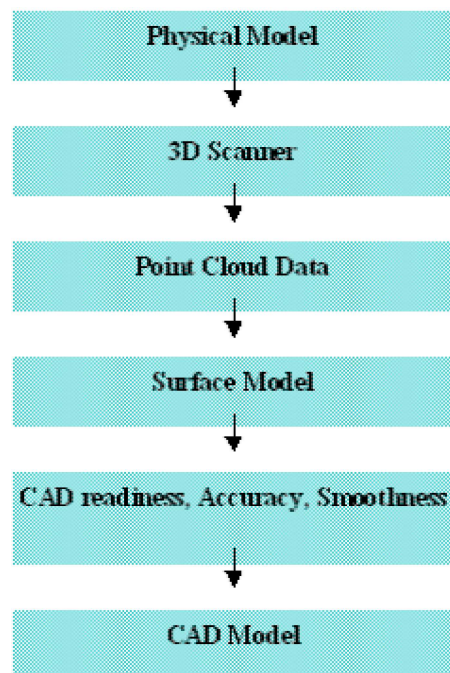


Figure 4.3: Reverse Engineering Methodology

4.2 Data Collection from Physical Part

With the help of reverse engineering one can make a CAD model of physical part of which drawing is not available. Computer model is created by digitization of already fabricated

model. Mapping of already existed product is done by acquisition of surface of the product either by contact or non- contact method. The file created contains many points in form of X, Y and Z coordinates on the product surface. There are two methods to obtain the data which are Contact method and Non-Contact method. As the name indicates, in contact method product is directly into the contact point of the measuring tool. In contact method, Generally the tool used is a probe or a stylus. In non-contact method light is used as the measuring tool to extract the data. Co-ordinate Measuring Machine or Sonic Digitizers used in case of contact method to detain co-ordinates of points on surface. In case of non-contact method white light or laser scanners are used to scan the object and create a 3-D model of the object. The selection of process is done on the behalf of parameters like speed and performance during digitization.

4.3 Principle of 3D Scanner

In 3D laser scanner laser light is used to review the model. In this scanner triangulation laser shines a laser on the object and deploys a camera to locate the laser the dots created by laser. Light emitted by laser, appears at the range of the camera's field of view. The position of laser dot, the laser emitter and camera form a triangle. Due to this position the technique is called triangulation. The length of one side of the triangle, the distance between the camera and the laser emitter is known. The angle of the laser emitter corner is also known. The angle of the camera corner can be determined by looking at the location of the laser dot in the camera's field of view. These three pieces of information fully determine the shape and size of the triangle and give the location of the laser dot corner of the triangle. In most cases a laser stripe, instead of a single laser dot, is swept across the object to speed up the acquisition process.

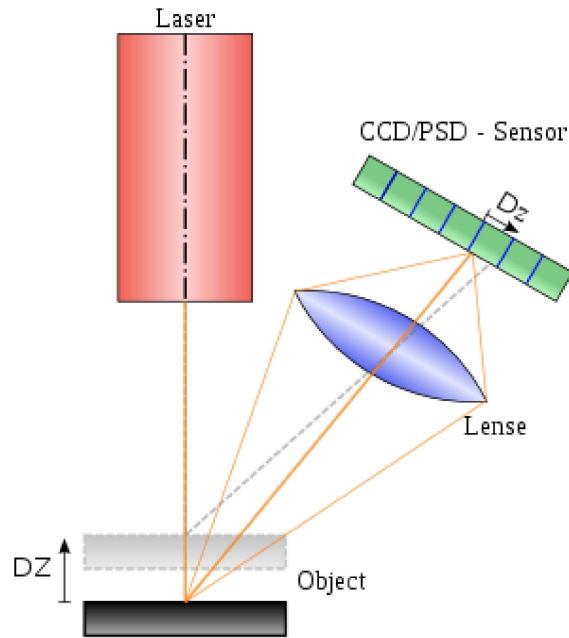


Figure 4.4: Principle of 3D Scanner [W5]

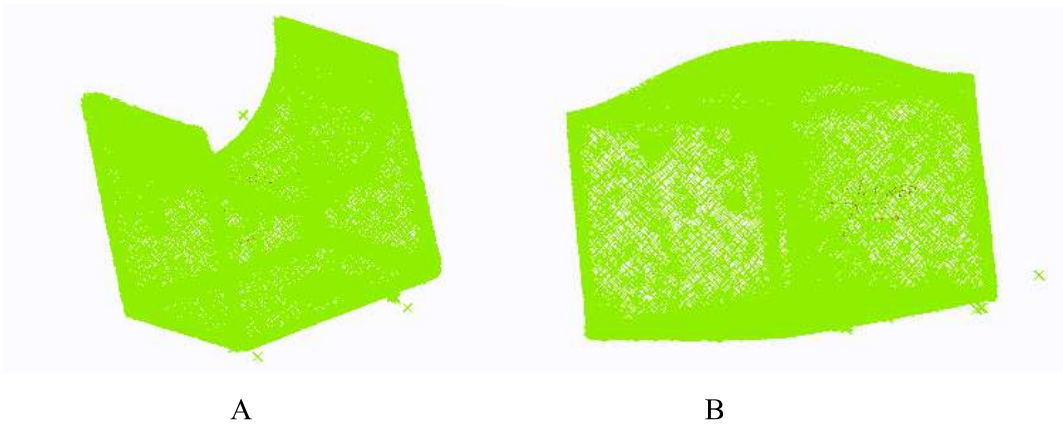
4.4 Generation of Parts

With the help of point cloud data generated by the 3D scanner the geometric model of the component could be obtained. When the CAD model is obtained from the that point cloud data the prototype of that model can be easily manufactured by FDM machine. These applications require feature extraction from the geometric model, followed by a process plan for the object, which involves definition of various manufacturing sequences required to manufacture the object. In the Figure, object is being captured with the help of the 3 D Scanner. As we know it is a light-based scanner, so a layer of white paint is being coated on the specimen to eliminate the reflection. It is not possible to take the graphical image without that layer of coating.



Figure 4.5: 3 D Scanner

The files generated by 3 D scanner are generally IGES files. The figures below show the point cloud data files created by the scanner.



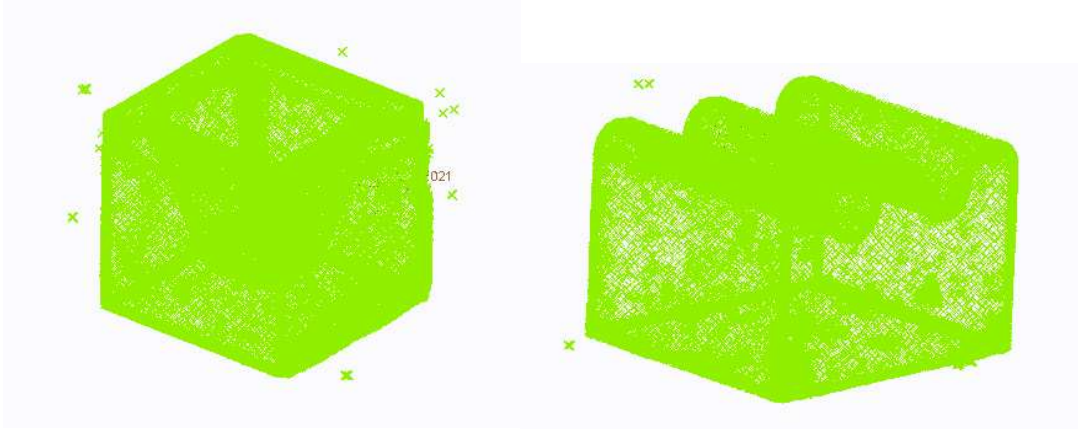


Figure 4.6: Point Cloud Files

C

D

4.5 Fabrication of Reverse Engineered Part

The main motive of collecting point cloud data was to fabricate a replica of the all the four parts so that the inspection could be proceeded. After collection, point cloud data has been converted stereolithography format, so that it could be fabricate through the rapid prototyping process. In PTC Creo Parametric 3.0 there is luxury to convert the file from .iges format to stereolithography(.stl). The transformation of the files from the .iges format to stereolithography format has been completed with the help of PTC Creo Parametric 3.0. After the conversion from .iges format to stereolithography format the models have been fabricated through the fused deposition modeling. Stratasys uPrint SE has been used to manufacture these models. The figure 4.7 shows the fabrication of the reverse engineered parts through the fused deposition modeling.

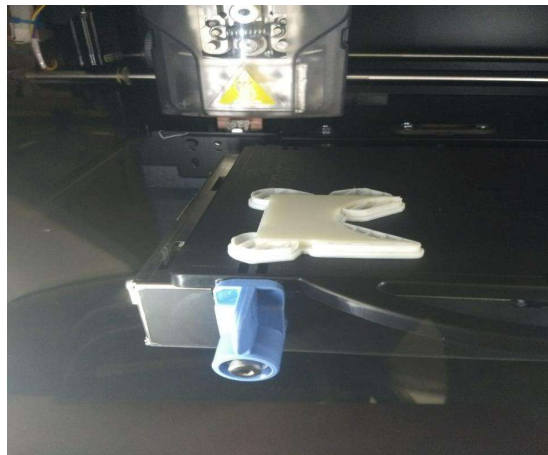


Figure 4.7: Fabrication of Reverse Engineered Part

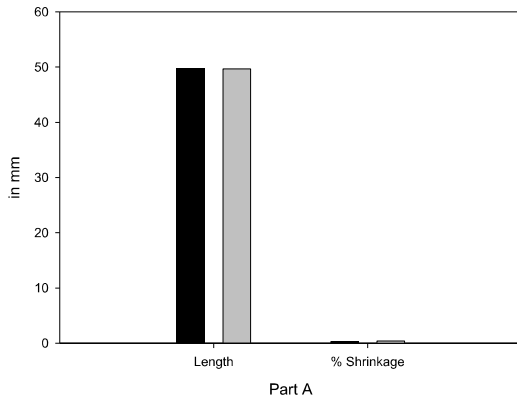
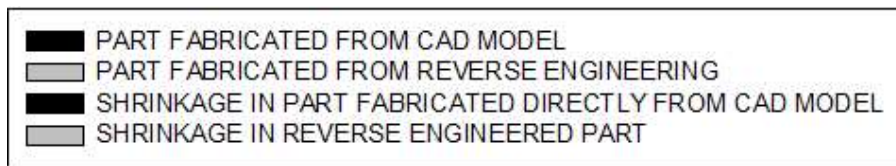
The number of points in the file created through reverse engineering are very much and some errors also occurs due to the coating of white paint provided before the scanning process. So, there are some errors in the file created through the reverse engineering.

CHAPTER 5: Comparative Analysis of Shrinkage for Parts

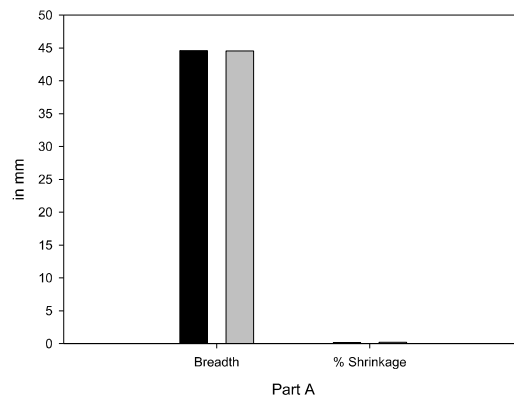
In this chapter, comparative analysis of shrinkage of parts fabricated by both the techniques have been proceeded. In starting of the experiment, parts have been manufactured directly through CAD model. After that RP parts have been fabricated through data collected with the help of reverse engineering. For ease in analysis, dimensions of each part have been fragmented into three segments. Length, breadth and height are the three segments which have been used during the analysis portion. Part A and D have some typical surface which contains diameters in their dimensions. Comparison between diameters of both parts has also been investigated. The brief information of the analysis is described through the charts.

5.1 Comparison of Various Parts

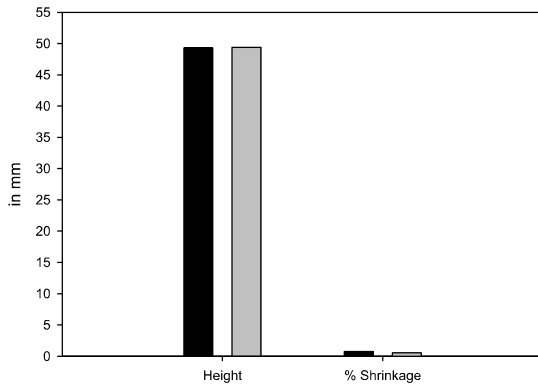
Analysis of Dimensions of PART (A):



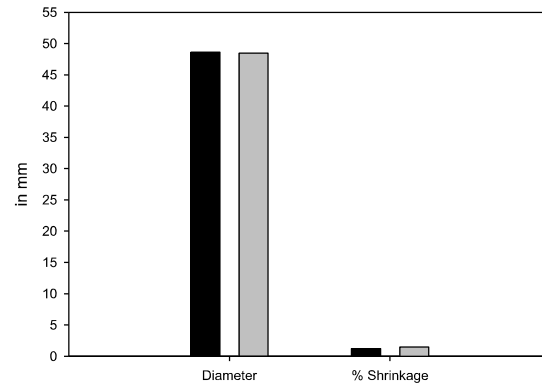
(5)



(b)



(c)

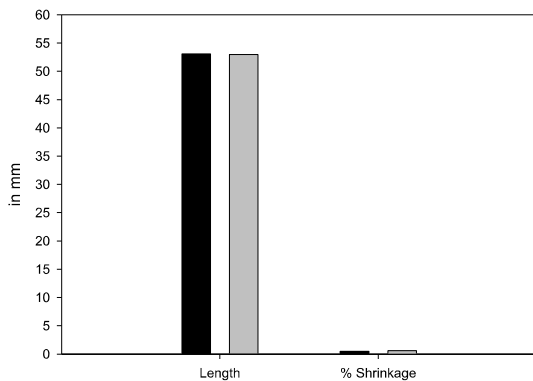
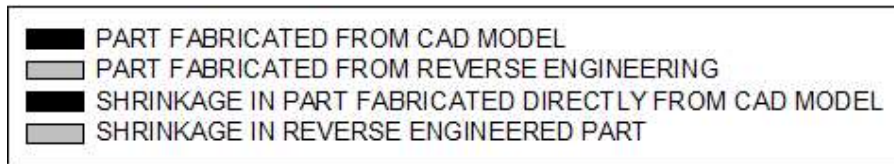


(d)

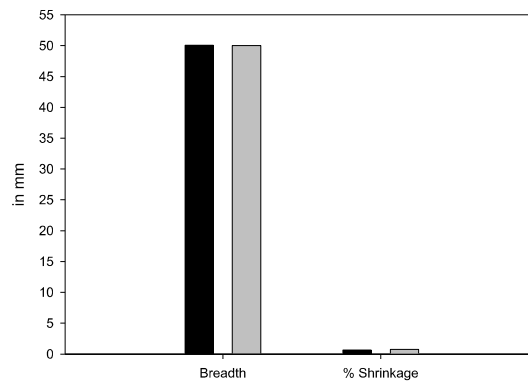
Figure 5.1: Dimensional Analysis of Part (A)

The investigation of part (A) confirms less shrinkage in terms of length, diameter and breadth in part fabricated through CAD model than the part fabricated through reverse engineering. Length of the CAD model was decrease by .26% where the amount of shrinkage in length of part manufactured by reverse engineering is .38%. While measurement of breadth, it has been noted that the shrinkage in CAD fabricated part is .13% where the shrinkage in RE part is .20%. But the trend is different the case of height where shrinkage in CAD part (.74%) is exceeding than shrinkage in reverse engineered part (.56%).

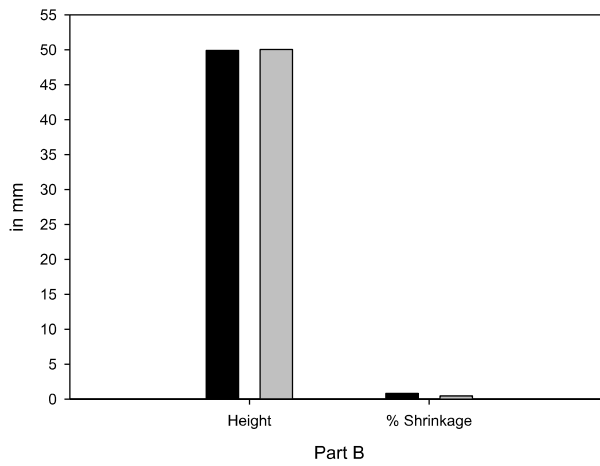
Analysis of Dimensions of PART (B):



(5)



(b)

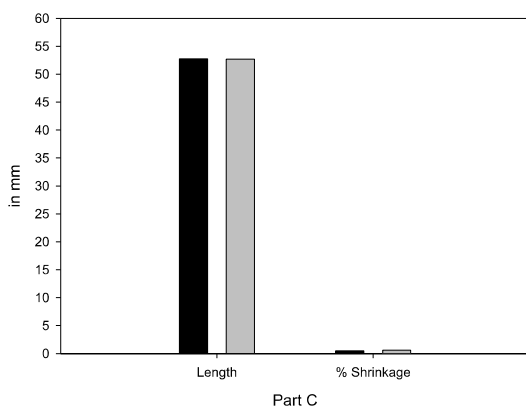
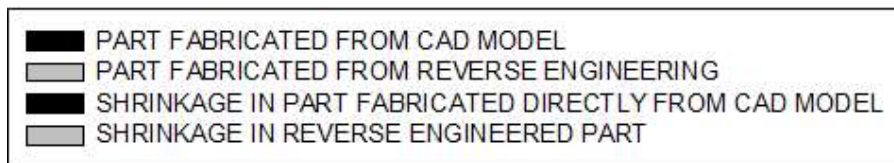


(c)

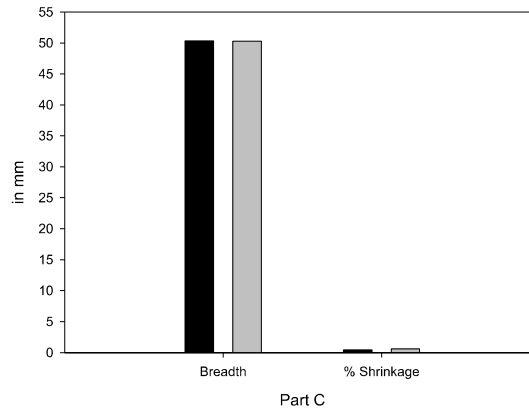
Figure 5.2 Dimensional Analysis of Part (B)

It has been noted during analysing both parts manufactured through different techniques, that the length in CAD model is decreased by .46% than the original dimension and length in reverse engineered part is reduced by .61%. Marginal reduction has been occurred in term of breadth in CAD model (.05%) and RE part (.01%). Shrinkage in height of CAD is .83% and in RE part is .49%.

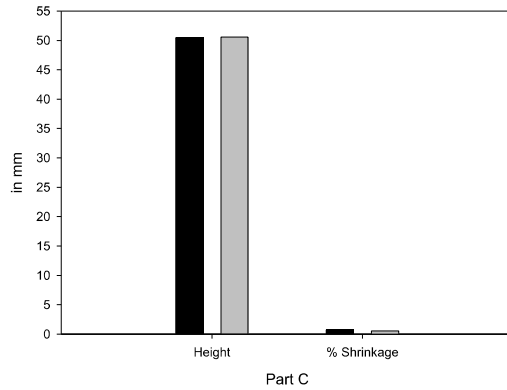
Analysis on Dimensions of PART ©:



(5)



(b)

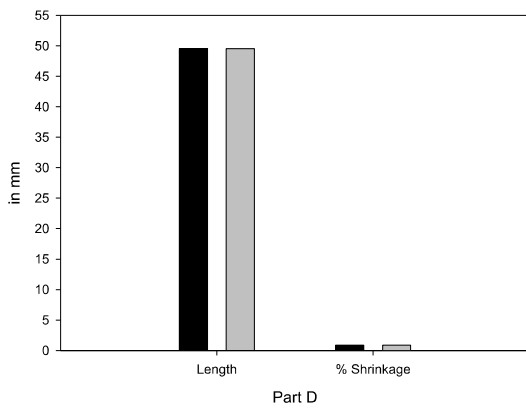
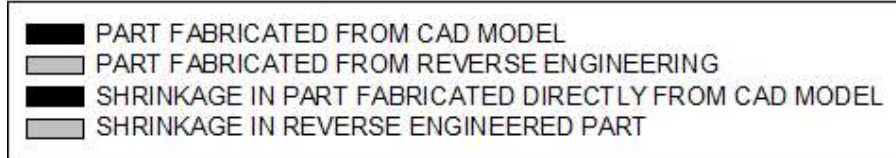


©

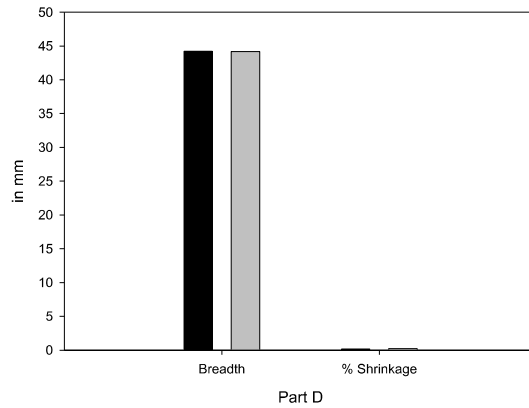
Figure 5.3 Dimensional Analysis of Part (C)

In Part (C), height of part is decreased by .47% in CAD model and .60% in RE Model. Breadth of CAD model is falls by .45%, where reduction of .61% is noted in RE model. Decline of height of part fabricated in RE (.53%) is less than the component made by CAD Model (.74%).

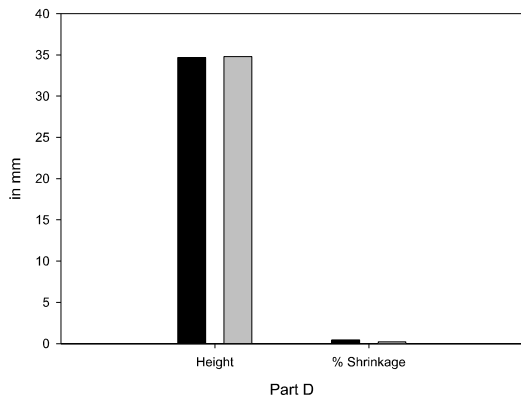
Analysis on Dimensions of PART (D):



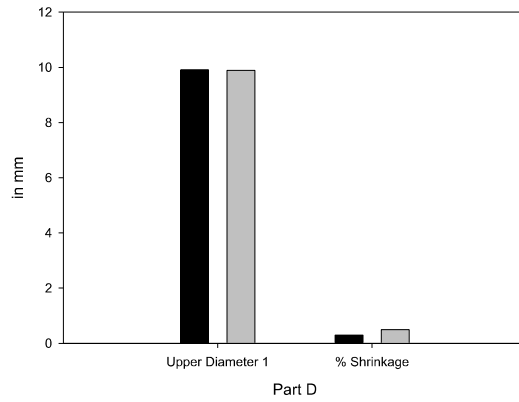
(a)



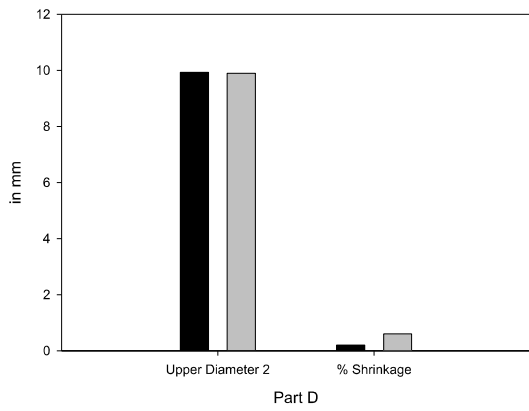
(b)



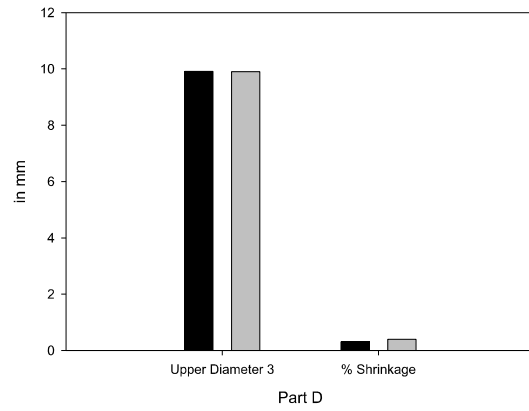
(c)



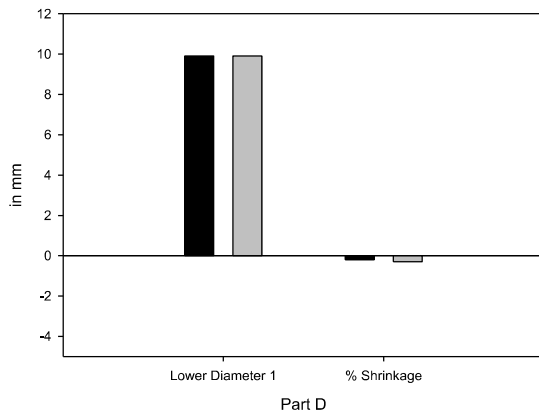
(d)



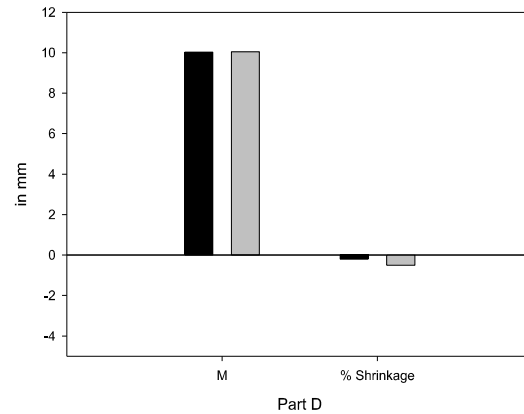
(e)



(f)



(g)



(h)

Figure 5.4 Dimensional Analysis of Part (D)

While investigation of part (D), it has been concluded that the shrinkage in length created with CAD model is .86% which is more precise than the part created by RE which is affected with .90% shrinkage. Shrinkage in breadth and height of the CAD fabricated part is .15% and .45% respectively. In RE fabricated part effect of shrinkage at breadth of the part is .22% and on height it is .20%.

After investigation of shrinkage in both the parts, it has been determined that there are more discrepancies in the part created with the help of reverse engineering than the part formed by direct CAD model. A trend of negative shrinkage has also been distinguished in case of inner diameters. Comparison is clearly indicating the dimensional inaccuracy in fabricated parts and the prime reason behind the inaccuracy is shrinkage. To tackle the problem of dimensional inaccuracy there is need of shrinkage compensation factor. In the next section designing of shrinkage compensation factor is described.

5.2 Designing of Shrinkage Compensation Factor

While designing shrinkage compensation factor, mean method formulation was applied to form the SCF. In the following table description of the formulation is provided.

Table 5.1: Mean of Change in Length of Parts

Part Name	Original Length (in mm)	Length of RP Part (in mm)	Change (in mm)
A	49.89	49.76	.13
B	53.31	53.06	.29
C	53	52.75	.25
D	49.98	49.55	.43

Mean of Change in Length of Parts:

$$A = \frac{1}{n} * \sum_{i=1}^n x_i$$

$$(0.13+0.29+0.25+0.43)/4= 0.27 \text{ mm}$$

Table 5.2: Mean of Change in Breadth of Parts

Part Name	Original Breadth (in mm)	Breadth of RP Part (in mm)	Change (in mm)
A	44.66	44.60	.06
B	50.40	50.07	.33
C	50.57	50.34	.23
D	44.27	44.20	.07

Mean of Change in Breadth of Parts:

$$(0.06+0.33+0.23+0.07)/4= 0.17 \text{ mm}$$

Table 5.3: Mean of Change in Height of Parts

Part Name	Original Height (in mm)	Height of RP Part (in mm)	Change (in mm)
A	49.63	49.26	.37
B	50.32	49.9	.42
C	50.84	50.46	.38
D	34.86	34.70	.16

Mean Change in Height of Parts:

$$(0.37+0.16+0.38+0.42)/4= 0.33 \text{ mm}$$

After reorganization of shrinkage in parts fabricated from RP, average change of dimensions in length, breadth and height is calculated. This average change of dimensions is considered as shrinkage compensation factor. For example, average change of length is 0.27 mm. In context of providing SCF to part, addition of 0.27 mm in the length is provided in the CAD model of the part. Similarly, same criteria are followed in respective parts to apply shrinkage compensation factor.

5.3 Fabrication of Parts Containing SCF

Shrinkage compensation factor is provided in model to tackle the dimensional inaccuracy formed due to shrinkage detained in the part. Shrinkage is formed in the part due to

phase change of the material during rapid prototyping process. Models containing SCF are created with the help of Stratasys uPrint SE. After fabrication, parts are inspected through coordinate measuring machine. In in next section detailed comparison of part is demonstrated.

5.4 Dimensional Analysis of Parts Containing SCF

To check dimensional accuracy of parts containing shrinkage compensation factor, part is compared and error in dimension is calculated. This comparison is illustrated with the help of vertical bars.

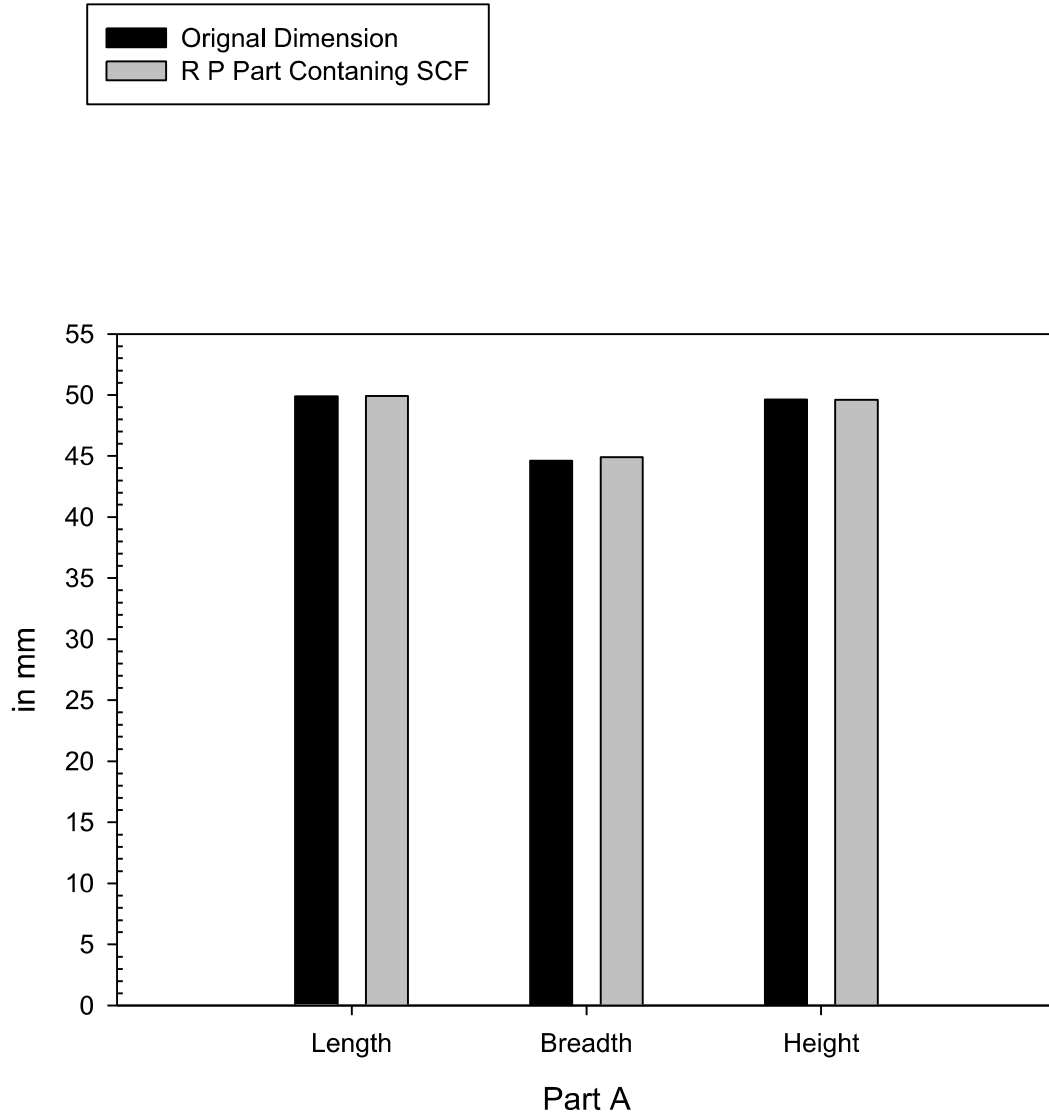


Figure 5.5: Comparison of part A

After analysing the part containing SCF, the study concludes that the shrinkage compensation factor designed through mean method is affective and fruitful to achieve the dimensional accuracy of the part. A marginal difference of .03 mm and .02 mm has been detected between

the reference part and SCF provided part. But in terms of breadth the difference between both the parts is .30 mm.

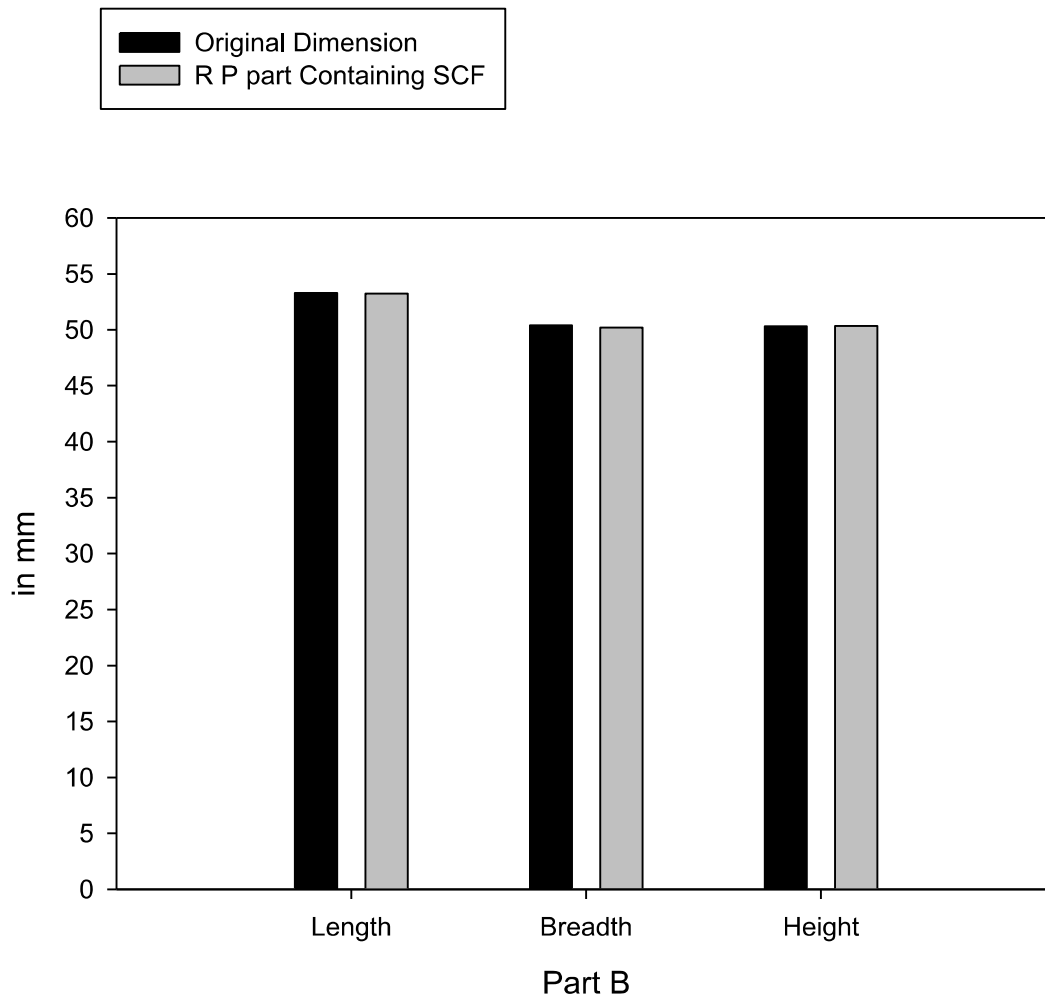


Figure 5.6: Comparison of part B

While checking dimensions of part B, the difference of .27 mm is notified in length, .17 mm in breadth and .16 mm in height. These results are much close to the reference value than the dimensions of parts with shrinkage compensation factor.

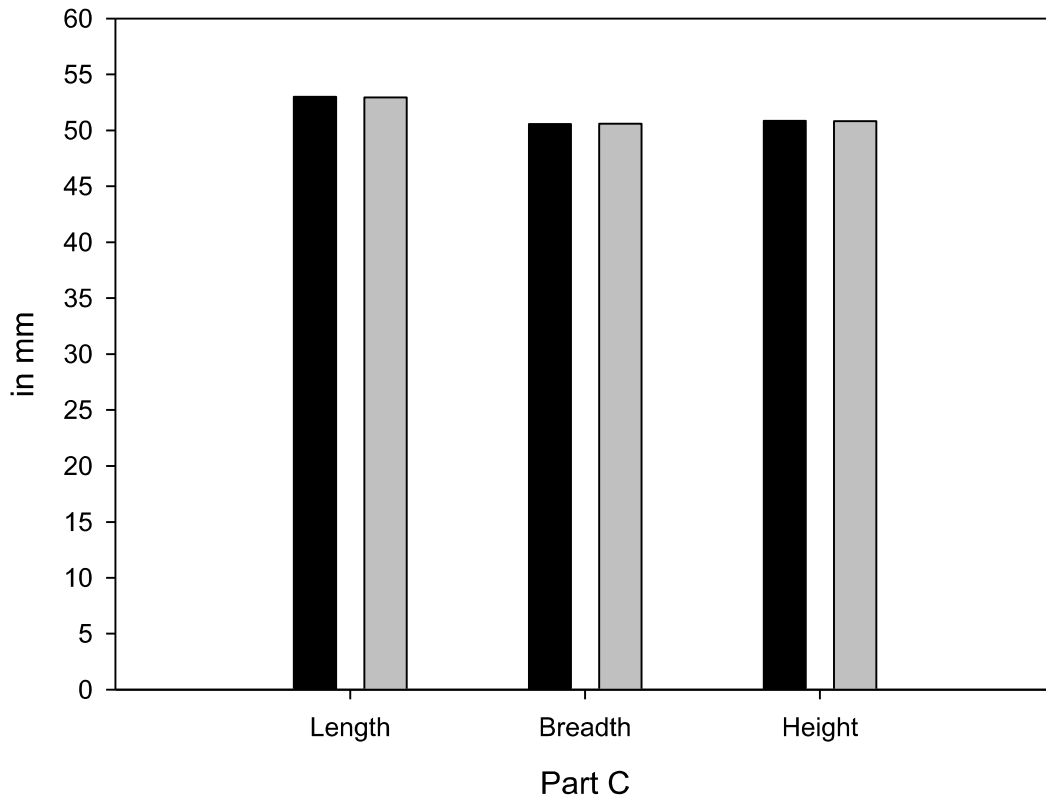


Figure 5.7: Comparison of Part C

Similarly, difference in part c between the length of the both parts is .27 mm. After analysing the dimensions of breadth and height the variance of .17 mm and .33 mm respectively is observed.

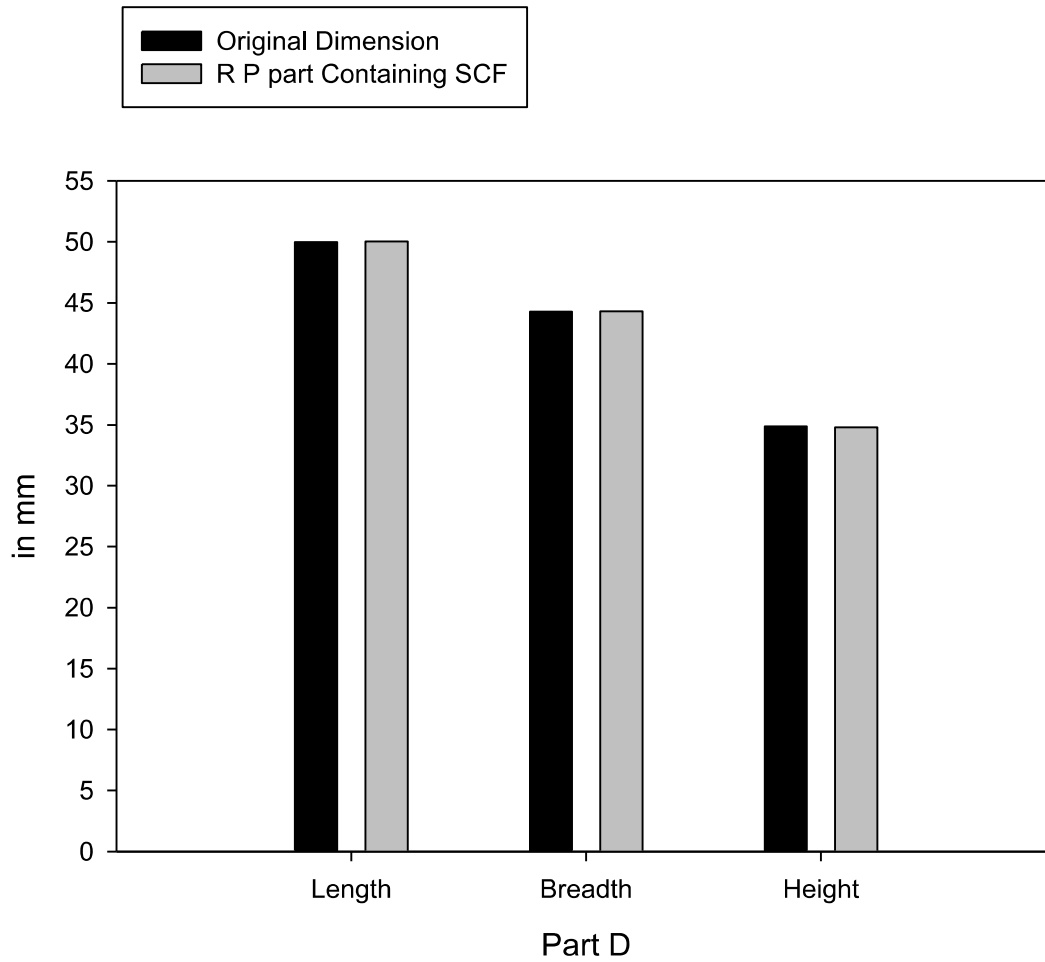


Figure 5.8: Comparison of Part D

Finally, in the last model a fringe variance of .07 mm is observed in the length of both the dimensions. In terms of breadth, the change between both the entities observed is of .34 mm. Difference noted between heights of both the dimensions is .29 mm.

5.5 STATISTICAL MODELLING OF SHRINKAGE FOR X DIRECTION LAYING

To study the effect of process parameters 20 experiments were performed. Layer thickness, part bed temperature and length of the specimen were considered for the inspection with three different values for each of the parameters described. Layer thickness of 0.1 mm, 0.2 mm and 0.3 mm have been inspected respectively. Part bed temperature have been taken as 111 °C, 113 °C and 115 °C. Length of 10 mm, 30 mm and 50 mm have been considered.

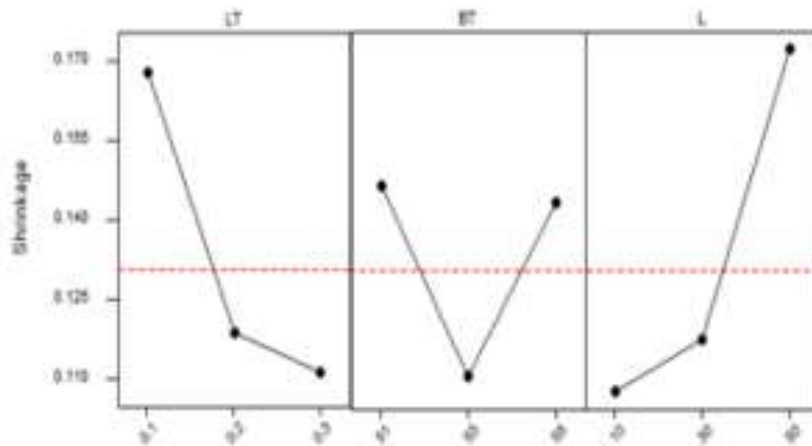


Figure 5.9: Main effect plot for shrinkage along the length in x direction

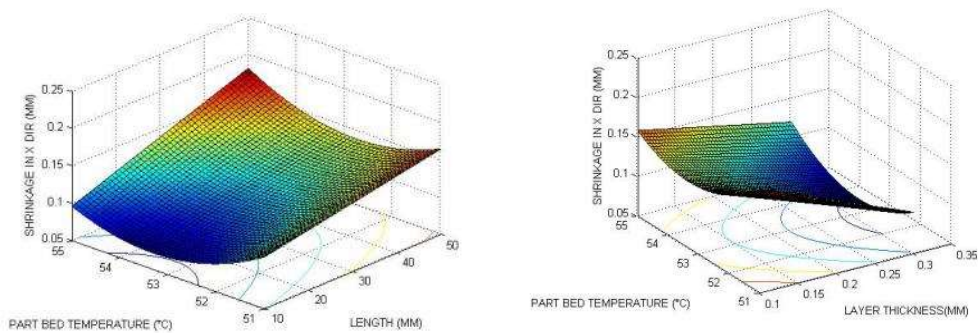


Figure 5.10: Response Surfaces for shrinkage for x direction laying along the length

It can be observed that the shrinkage decreases with increase in layer thickness. In FDM, conduction and forced convection are the modes of heat dissipation. These processes reduce the temperature thereby, forcing the material to solidify in less time. It is observed that bonding between the filaments occurs due to re-melting and diffusion of previous layer. This results in uneven temperature fluctuations, thereby developing non-uniform temperature gradients. It is observed that shrinkage increases with an increase in length of the parts. The increase in shrinkage can be attributed to development of more internal stresses with increase in length, resulting from the contraction of depositing fibres. It has been reported that the deposited thermoplastic fibre is subjected to contraction when cooled from extrusion temperature to glass transition temperature.

Figure below shows the main effect plot of shrinkage along the height in x direction laying. These three points are obtained from the experimental data, which are calculated based on average of sum of response containing the processing conditions. Shrinkage decrease with increase in layer thickness.

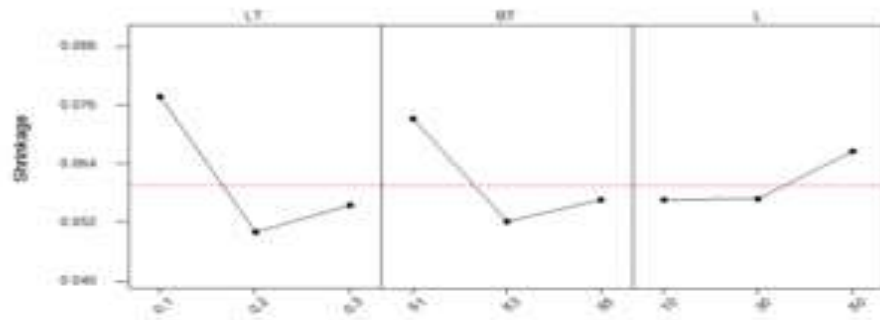


Figure 5.11: Main effect plot for shrinkage along the width in x direction laying

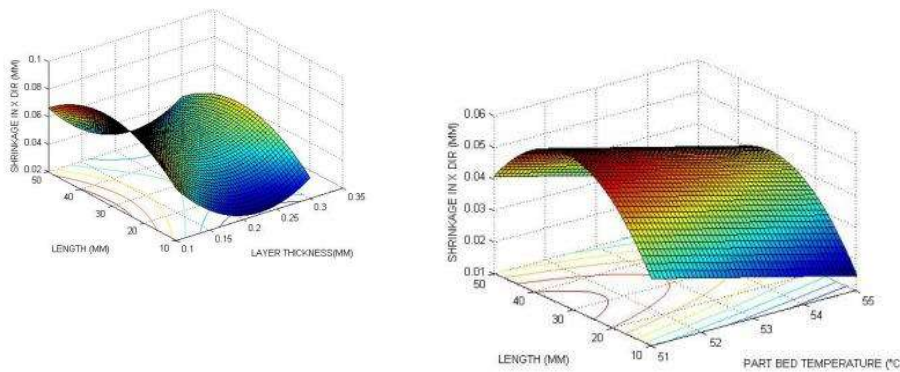


Figure 5.12: Response Surfaces for shrinkage for x direction laying along the width

The effect of nozzle diameter on shrinkage along the width is highlighted in Figure 40. As the nozzle diameter is increased, it is observed that shrinkage also increases. This may be due to more volume of material being deposited with increase in width results in greater internal stresses and hence more contraction.

Figure below shows the main effect plot of shrinkage along the height in x direction laying. These three points are obtained from the experimental data, which are calculated based on average of sum of response containing the processing conditions. Shrinkage decrease with increase in layer thickness.

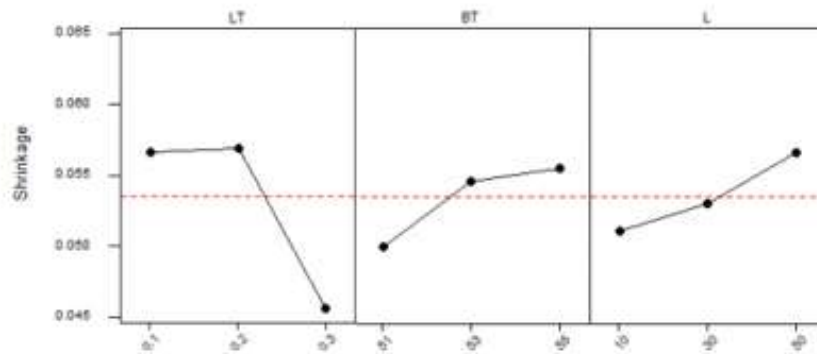


Figure 5.13: Response Surfaces for shrinkage for x direction laying along the Height

Figure shows the surface and contour plots for the shrinkage drawn using equation 8. It is observed that, surface contour provides avenue for interpreting the surface design.

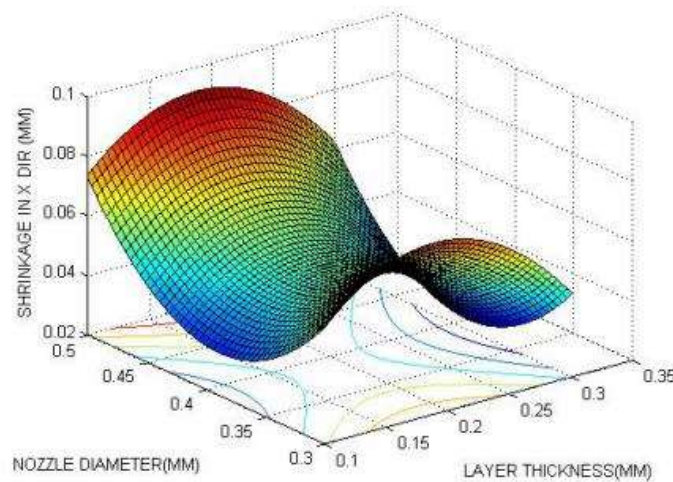


Figure 5.14: Response Surfaces for shrinkage for x direction laying along the Height

Conclusions

The main objective of this study was to develop discreet process planning guidelines to enhance the accuracy of the part fabricated by Fuse Deposition Modeling (FDM). The study included the effect of shrinkage on the part manufactured by reverse engineering.

In experimentation, shrinkage compensation factor was developed to overcome the shrinkage occurred due to phase change of the material. Shrinkage compensation factor (SCF) was developed on the base of mean method to improve the overall accuracy of the part. Further, through various experiments, process planning guidelines were designed to enhance the accuracy of the part. Besides, the guidelines were established and confirmed by specific fabricating parts constituting of shrinkage compensation factor. Further, the expected quality of the fabricated parts was counted with respect to each guideline.

The two parts developed in this study were created from two distinct methodologies:

- a. Through reverse engineering: This was done with the help of a 3D scanner by which point cloud data was obtained. This point cloud data was converted into a stereolithographic format. Further, through the stereolithographic information, ABS parts were developed using FDM Stratasys uPrint.
- b. Through CAD modelling: In this method, CMM was used to fetch the dimensions of the typical surfaces. Based on the dimensions, a CAD model was constructed on the PTC Creo 3.0. These CAD models were converted into the stereolithographic format to finally obtain the ABS parts through Stratasys uPrint.

The results from the comparison of the both the parts obtained by different methodologies showed that accuracy of CAD modelling is higher in comparison to the reverse engineering methods if length and breadth of the parts is considered. However, if height of the parts were considered then the accuracy of the reverse engineering method was higher.

The results also signified that in the case of the reverse engineering method, an additional paint coating was required to minimize the light deformation error in the 3D Scanner. However, the additional paint coating reduced the surface finishing of the parts.

Conclusively, the results of the research presented efficient guidelines which would be fruitful for both the process planner and the product designer, equally.

Future Scope

Future work lies in several areas of RP processes.

1. First and foremost, it is required to find out further guidelines which will help in improving the quality of part. The guidelines presented in this work are not all-encompassing list, further guidelines are needed to be identified and can be validated by the methodology developed in this study.
2. Further examination of the interactions of the process parameters on the guidelines is needed to be study. Correlating the guidelines is a crucial area where the further research is required. By determining the interactions and correlations between the guidelines, further refinement can be done.
3. Another possible concern is that there might be a point when two different guidelines cannot be simultaneously applied on the same part. If this scenario occurs, further examination is required to identify the most beneficial guideline and an order of preference should be decided according to quality attribute of the part.

With many further areas of research is defined, the refining of the guidelines for the FDM is a significant task. This area of research will help in improving the quality attributes of the parts fabricated from FDM like strength and accuracy of the part and can assist FDM to become a full-scale manufacturing process.

References

1. Chua, C.K., Leong, K.F et al, “Rapid Prototyping – Principles and Applications”, 3rd ed. World Scientific Publishing Co. Pte. Ltd., Singapore.
2. Gibson, I., Rosen, D. and Stucker, B., 2014. Additive manufacturing technologies: 3D printing, Rapid Prototyping , and direct digital manufacturing. Springer.
3. Borille, A., Gomes, J., Meyer, R. and Grote, K., 2010. Applying decision methods to select Rapid Prototyping technologies. *Rapid Prototyping Journal*, 16(1), pp.50-62
4. Kodama, H., 1981. Automatic method for fabricating a three-dimensional plastic model with photo-hardening polymer. *Review of scientific instruments*, 52(11), pp.1770-1773.
5. Hull, C.W., Uvp, Inc., 1986. Apparatus for production of three-dimensional objects by stereolithography. U.S. Patent 4,575,330
6. Mahindru, D.V., Priyanka Mahendru, S.R.M.G.P.C. and Ganj, T., 2013. Review of Rapid Prototyping -technology for the future. *Global Journal of Computer Science and Technology*, 13(4).
7. Lee, K.S., Kim, R.H., Yang, D.Y. and Park, S.H., 2008. Advances in 3D nano/microfabrication using two-photon initiated polymerization. *Progress in Polymer Science*, 33(6), pp.631-681
8. Pham, D.T. and Gault, R.S., 1998. A comparison of Rapid Prototyping technologies. *International Journal of machine tools and manufacture*, 38(10), pp.1257- 1287.
9. Lü, L., Fuh, J. and Wong, Y.S., 2013. Laser-induced materials and processes for Rapid Prototyping . Springer Science & Business Media
10. Soe, S.P., 2012. Quantitative analysis on SLS part curling using EOS P700 machine. *Journal of Materials Processing Technology*, 212(11), pp.2433-2442.
11. Rayna, T., & Striukova, L. (2016). From rapid prototyping to home fabrication: How 3D printing is changing business model innovation. *Technological Forecasting and Social Change*, 102, 214-224.
12. Fischer, J. (2012). *Handbook of molded part shrinkage and warpage*. William Andrew.
13. Perez, A. R. T., Roberson, D. A., & Wicker, R. B. (2014). Fracture surface analysis of 3D-printed tensile specimens of novel ABS-based materials. *Journal of Failure Analysis and Prevention*, 14(3), 343-353.
14. Baich, L., & Manogharan, G. (2015). Study of infill print parameters on mechanical strength and production cost-time of 3D printed ABS parts. In *International Solid Freeform Fabrication Symposium*, Austin, TX (pp. 209-2018).

15. Hernandez, R., Slaughter, D., Whaley, D., Tate, J., & Asiabanpour, B. Analysing the tensile, compressive, and flexural properties of 3D printed ABS P430 plastic based on printing orientation using fused deposition modeling.
16. Boschetto, A., & Bottini, L. (2014). Accuracy prediction in fused deposition modeling. *The international journal of advanced manufacturing technology*, 73(5-8), 913-928.
17. Kulkarni, P. and Dutta, D., 1999. Deposition strategies and resulting part stiffnesses in fused deposition modeling. *Journal of manufacturing science and engineering*, 121(1), pp.93-103.
18. Masood, S.H. and Song, W.Q., 2004. Development of new metal/polymer materials for Rapid Tooling using fused deposition modeling. *Materials & Design*, 25(7), pp.587-594.
19. Lee, K. H., & Woo, H. (2000). Direct integration of reverse engineering and rapid prototyping. *Computers & Industrial Engineering*, 38(1), 21-38.
20. Paulic, M., Irgolic, T., Balic, J., Cus, F., Cupar, A., Brajljih, T., & Drstvensek, I. (2014). Reverse engineering of parts with optical scanning and additive manufacturing. *Procedia Engineering*, 69, 795-803.
21. Xu, Y. (2016). Experimental Study of ABS Material Shrinkage and Deformation Based on Fused Deposition Modeling. In *MATEC Web of Conferences* (Vol. 67, p. 03039). EDP Sciences.
22. Wang, T. M., Xi, J. T., & Jin, Y. (2007). A model research for prototype warp deformation in the FDM process. *The International Journal of Advanced Manufacturing Technology*, 33(11), 1087-1096.
23. Huang, Y. M., & Lan, H. Y. (2006). Path planning effect for the accuracy of rapid prototyping system. *The International Journal of Advanced Manufacturing Technology*, 30(3), 233-246.
24. Senthilkumaran, K., Pulak Mohan Pandey, and PV Madhusudan Rao. "Shrinkage compensation along single direction dixel space for improving accuracy in selective laser sintering." *Automation Science and Engineering*, 2008. CASE 2008. IEEE International Conference on. IEEE, 2008.
25. Schmutzler, C., Zimmermann, A., & Zaeh, M. F. (2016). Compensating warpage of 3D printed parts using free-form deformation. *Procedia CIRP*, 41, 1017-1022.
26. Dao, Q., Frimodig, J. C., Le, H. N., Li, X. Z., Putnam, S. B., Golda, K., ... & Fritz, B. (1999). Calculation of shrinkage compensation factors for rapid prototyping (FDM 1650). *Computer Applications in engineering education*, 7(3), 186-195.

27. Pandey, P. M., Reddy, N. V., & Dhande, S. G. (2003). Improvement of surface finish by staircase machining in fused deposition modeling. *Journal of materials processing technology*, 132(1), 323-331.
28. Nosouhi, R.; Rahmati, S. (2010) Finite Element Analysis of Shrinkage Phenomena in Stereolithography and Development of a New Hatching Method. 10th Iranian Conference on Manufacturing Engineering, ICME.
29. Williams, J. D.; Deckard, C. R.; (1998) Advances in modeling the effects of selected parameters on the SLS process. *Rapid Prototyping Journal* 4, no. 2, 90-100
30. Gregorian, A.; Elliot, B.; Navarro, R.; Ochoa, F.; Singh, H.; Monge, E.; Foyos, J.; Noorani, R.; Fritz, B.; Jayanthi, S. (2001) Accuracy improvement in rapid prototyping machine (FDM-1650). In *Solid Freeform Fabrication Proceedings*, pp. 77-84.

Web References

W1. <https://www.livescience.com/40310-laminated-object-manufacturing.html>

(Accessed on March 2018)

W2. <https://www.3dhubs.com/what-is-3d-printing>

(Accessed on April 2018)

W3. <https://www.emeraldinsight.com/doi/abs/10.1108/13552541211250364>

(Accessed on April 2018)

W4. https://en.wikipedia.org/wiki/Coordinate-measuring_machine

(Accessed on May 2018)

W5. https://en.wikipedia.org/wiki/3D_scanner

(Accessed on May 2018)

Annexure 1

%	N134 Y29. Z-0.1717	N186 G03 X20.106 Y29. Z-1.2458 I20.106 J-4.
O1000 (PRT000123)	N136 X-20.106 Z-0.1798	N188 G01 X29. Z-1.2543
N100 (COMPENSATION- WEAR)	N138 G03 X20.106 Y29. Z-0.246 I20.106 J-4.	N190 Y-29. Z-1.3091
N102 (REV-0.70)	N140 G01 X29. Z-0.2543	N192 X-29. Z-1.364
N104 (OCT-30-2017- 1:54:53PM)	N142 Y-29. Z-0.3091	N194 Y29. Z-1.4189
	N144 X-29. Z-0.364	N196 X-20.106 Z-1.4273
	N146 Y29. Z-0.4189	N198 G03 X20.106 Y29. Z-1.4958 I20.106 J-4.
	N148 X-20.106 Z-0.4273	N200 G01 X29. Z-1.5043
N106 (TOOL 1 - DIA 8.)	N150 G03 X20.106 Y29. Z-0.4958 I20.106 J-4.	N202 Y-29. Z-1.5591
	N152 G01 X29. Z-0.5043	N204 X-29. Z-1.614
	N154 Y-29. Z-0.5591	N206 Y29. Z-1.6689
N1 G90 G17 G40 G80 G00	N156 X-29. Z-0.614	N208 X-20.106 Z-1.6773
N108 M06 T1 ()	N158 Y29. Z-0.6689	N210 G03 X20.106 Y29. Z-1.7458 I20.106 J-4.
N110 (F-contour)	N160 X-20.106 Z-0.6773	N212 G01 X29. Z-1.7543
N112 G00 G54 G90 X18.751 Y35. S3979 M03	N162 G03 X20.106 Y29. Z-0.7458 I20.106 J-4.	N214 Y-29. Z-1.8091
N114 G43 H1 Z120.	N164 G01 X29. Z-0.7543	N216 X-29. Z-1.864
N116 S4000	N166 Y-29. Z-0.8091	N218 Y29. Z-1.9189
N118 Z25.	N168 X-29. Z-0.864	N220 X-20.106 Z-1.9273
N120 Z2.	N170 Y29. Z-0.9189	N222 G03 X20.106 Y29. Z-1.9958 I20.106 J-4.
N122 G01 Z0. F400.	N172 X-20.106 Z-0.9273	N224 G01 X29. Z-2.0043
N124 G41 D1 X18.5 F800.	N174 G03 X20.106 Y29. Z-0.9958 I20.106 J-4.	N226 Y-29. Z-2.0591
N126 G03 X24.5 Y29. Z- 0.0086 I6. J0.	N176 G01 X29. Z-1.0043	N228 X-29. Z-2.114
N128 G01 X29. Z-0.0127	N178 Y-29. Z-1.0591	N230 Y29. Z-2.1689
N130 Y-29. Z-0.0657	N180 X-29. Z-1.114	N232 X-20.106 Z-2.1773
N132 X-29. Z-0.1187	N182 Y29. Z-1.1689	N234 G03 X20.106 Y29. Z-2.2458 I20.106 J-4.
	N184 X-20.106 Z-1.1773	

N236 G01 X29. Z-2.2543	N292 X-20.106 Z-3.4273	N346 Y-29. Z-4.5591
N238 Y-29. Z-2.3091	N294 G03 X20.106 Y29. Z-3.4958 I20.106 J-4.	N348 X-29. Z-4.614
N240 X-29. Z-2.364	N296 G01 X29. Z-3.5043	N350 Y29. Z-4.6689
N242 Y29. Z-2.4189	N298 Y-29. Z-3.5591	N352 X-20.106 Z-4.6773
N244 X-20.106 Z-2.4273	N300 X-29. Z-3.614	N354 G03 X20.106 Y29. Z-4.7458 I20.106 J-4.
N246 G03 X20.106 Y29. Z-2.4958 I20.106 J-4.	N302 Y29. Z-3.6689	N356 G01 X29. Z-4.7543
N248 G01 X29. Z-2.5043	N304 X-20.106 Z-3.6773	N358 Y-29. Z-4.8091
N250 Y-29. Z-2.5591	N306 G03 X20.106 Y29. Z-3.7458 I20.106 J-4.	N360 X-29. Z-4.864
N252 X-29. Z-2.614	N308 G01 X29. Z-3.7543	N362 Y29. Z-4.9189
N254 Y29. Z-2.6689	N310 Y-29. Z-3.8091	N364 X-20.106 Z-4.9273
N256 X-20.106 Z-2.6773	N312 X-29. Z-3.864	N366 G03 X20.106 Y29. Z-4.9958 I20.106 J-4.
N258 G03 X20.106 Y29. Z-2.7458 I20.106 J-4.	N314 Y29. Z-3.9189	N368 G01 X29. Z-5.0043
N260 G01 X29. Z-2.7543	N316 X-20.106 Z-3.9273	N370 Y-29. Z-5.0591
N262 Y-29. Z-2.8091	N318 G03 X20.106 Y29. Z-3.9958 I20.106 J-4.	N372 X-29. Z-5.114
N264 X-29. Z-2.864	N320 G01 X29. Z-4.0043	N374 Y29. Z-5.1689
N266 Y29. Z-2.9189	N322 Y-29. Z-4.0591	N376 X-20.106 Z-5.1773
N268 X-20.106 Z-2.9273	N324 X-29. Z-4.114	N378 G03 X20.106 Y29. Z-5.2458 I20.106 J-4.
N270 G03 X20.106 Y29. Z-2.9958 I20.106 J-4.	N326 Y29. Z-4.1689	N380 G01 X29. Z-5.2543
N272 G01 X29. Z-3.0043	N328 X-20.106 Z-4.1773	N382 Y-29. Z-5.3091
N274 Y-29. Z-3.0591	N330 G03 X20.106 Y29. Z-4.2458 I20.106 J-4.	N384 X-29. Z-5.364
N276 X-29. Z-3.114	N332 G01 X29. Z-4.2543	N386 Y29. Z-5.4189
N278 Y29. Z-3.1689	N334 Y-29. Z-4.3091	N388 X-20.106 Z-5.4273
N280 X-20.106 Z-3.1773	N336 X-29. Z-4.364	N390 G03 X20.106 Y29. Z-5.4958 I20.106 J-4.
N282 G03 X20.106 Y29. Z-3.2458 I20.106 J-4.	N338 Y29. Z-4.4189	N392 G01 X29. Z-5.5043
N284 G01 X29. Z-3.2543	N340 X-20.106 Z-4.4273	N394 Y-29. Z-5.5591
N286 Y-29. Z-3.3091	N342 G03 X20.106 Y29. Z-4.4958 I20.106 J-4.	N396 X-29. Z-5.614
N288 X-29. Z-3.364	N344 G01 X29. Z-4.5043	N398 Y29. Z-5.6689
N290 Y29. Z-3.4189		N400 X-20.106 Z-5.6773

N402 G03 X20.106 Y29. Z-5.7458 I20.106 J-4.	N456 X-29. Z-6.864	N510 G03 X20.106 Y29. Z-7.9958 I20.106 J-4.
N404 G01 X29. Z-5.7543	N458 Y29. Z-6.9189	N512 G01 X29. Z-8.0043
N406 Y-29. Z-5.8091	N460 X-20.106 Z-6.9273	N514 Y-29. Z-8.0591
N408 X-29. Z-5.864	N462 G03 X20.106 Y29. Z-6.9958 I20.106 J-4.	N516 X-29. Z-8.114
N410 Y29. Z-5.9189	N464 G01 X29. Z-7.0043	N518 Y29. Z-8.1689
N412 X-20.106 Z-5.9273	N466 Y-29. Z-7.0591	N520 X-20.106 Z-8.1773
N414 G03 X20.106 Y29. Z-5.9958 I20.106 J-4.	N468 X-29. Z-7.114	N522 G03 X20.106 Y29. Z-8.2458 I20.106 J-4.
N416 G01 X29. Z-6.0043	N470 Y29. Z-7.1689	N524 G01 X29. Z-8.2543
N418 Y-29. Z-6.0591	N472 X-20.106 Z-7.1773	N526 Y-29. Z-8.3091
N420 X-29. Z-6.114	N474 G03 X20.106 Y29. Z-7.2458 I20.106 J-4.	N528 X-29. Z-8.364
N422 Y29. Z-6.1689	N476 G01 X29. Z-7.2543	N530 Y29. Z-8.4189
N424 X-20.106 Z-6.1773	N478 Y-29. Z-7.3091	N532 X-20.106 Z-8.4273
N426 G03 X20.106 Y29. Z-6.2458 I20.106 J-4.	N480 X-29. Z-7.364	N534 G03 X20.106 Y29. Z-8.4958 I20.106 J-4.
N428 G01 X29. Z-6.2543	N482 Y29. Z-7.4189	N536 G01 X29. Z-8.5043
N430 Y-29. Z-6.3091	N484 X-20.106 Z-7.4273	N538 Y-29. Z-8.5591
N432 X-29. Z-6.364	N486 G03 X20.106 Y29. Z-7.4958 I20.106 J-4.	N540 X-29. Z-8.614
N434 Y29. Z-6.4189	N488 G01 X29. Z-7.5043	N542 Y29. Z-8.6689
N436 X-20.106 Z-6.4273	N490 Y-29. Z-7.5591	N544 X-20.106 Z-8.6773
N438 G03 X20.106 Y29. Z-6.4958 I20.106 J-4.	N492 X-29. Z-7.614	N546 G03 X20.106 Y29. Z-8.7458 I20.106 J-4.
N440 G01 X29. Z-6.5043	N494 Y29. Z-7.6689	N548 G01 X29. Z-8.7543
N442 Y-29. Z-6.5591	N496 X-20.106 Z-7.6773	N550 Y-29. Z-8.8091
N444 X-29. Z-6.614	N498 G03 X20.106 Y29. Z-7.7458 I20.106 J-4.	N552 X-29. Z-8.864
N446 Y29. Z-6.6689	N500 G01 X29. Z-7.7543	N554 Y29. Z-8.9189
N448 X-20.106 Z-6.6773	N502 Y-29. Z-7.8091	N556 X-20.106 Z-8.9273
N450 G03 X20.106 Y29. Z-6.7458 I20.106 J-4.	N504 X-29. Z-7.864	N558 G03 X20.106 Y29. Z-8.9958 I20.106 J-4.
N452 G01 X29. Z-6.7543	N506 Y29. Z-7.9189	N560 G01 X29. Z-9.0043
N454 Y-29. Z-6.8091	N508 X-20.106 Z-7.9273	N562 Y-29. Z-9.0591

N564 X-29. Z-9.114	N616 X-20.106 Z-10.1773	N662 Y29. Z-11.1689
N566 Y29. Z-9.1689	N618 G03 X20.106 Y29. Z-10.2458 I20.106 J-4.	N664 X-20.106 Z-11.1773
N568 X-20.106 Z-9.1773	N620 G01 X29. Z-10.2543	N666 G03 X20.106 Y29. Z-11.2458 I20.106 J-4.
N570 G03 X20.106 Y29. Z-9.2458 I20.106 J-4.	N622 Y-29. Z-10.3091	N668 G01 X29. Z-11.2543
N572 G01 X29. Z-9.2543	N624 X-29. Z-10.364	N670 Y-29. Z-11.3091
N574 Y-29. Z-9.3091	N626 Y29. Z-10.4189	N672 X-29. Z-11.364
N576 X-29. Z-9.364	N628 X-20.106 Z-10.4273	N674 Y29. Z-11.4189
N578 Y29. Z-9.4189	N630 G03 X20.106 Y29. Z-10.4958 I20.106 J-4.	N676 X-20.106 Z-11.4273
N580 X-20.106 Z-9.4273	N632 G01 X29. Z-10.5043	N678 G03 X20.106 Y29. Z-11.4958 I20.106 J-4.
N582 G03 X20.106 Y29. Z-9.4958 I20.106 J-4.	N634 Y-29. Z-10.5591	N680 G01 X29. Z-11.5043
N584 G01 X29. Z-9.5043	N636 X-29. Z-10.614	N682 Y-29. Z-11.5591
N586 Y-29. Z-9.5591	N638 Y29. Z-10.6689	N684 X-29. Z-11.614
N588 X-29. Z-9.614	N640 X-20.106 Z-10.6773	N686 Y29. Z-11.6689
N590 Y29. Z-9.6689	N642 G03 X20.106 Y29. Z-10.7458 I20.106 J-4.	N688 X-20.106 Z-11.6773
N592 X-20.106 Z-9.6773	N644 G01 X29. Z-10.7543	N690 G03 X20.106 Y29. Z-11.7458 I20.106 J-4.
N594 G03 X20.106 Y29. Z-9.7458 I20.106 J-4.	N646 Y-29. Z-10.8091	N692 G01 X29. Z-11.7543
N596 G01 X29. Z-9.7543	N648 X-29. Z-10.864	N694 Y-29. Z-11.8091
N598 Y-29. Z-9.8091	N650 Y29. Z-10.9189	N696 X-29. Z-11.864
N600 X-29. Z-9.864	N652 X-20.106 Z-10.9273	N698 Y29. Z-11.9189
N602 Y29. Z-9.9189	N654 G03 X20.106 Y29. Z-10.9958 I20.106 J-4.	N700 X-20.106 Z-11.9273
N604 X-20.106 Z-9.9273	N656 G01 X29. Z-11.0043	N702 G03 X20.106 Y29. Z-11.9958 I20.106 J-4.
N606 G03 X20.106 Y29. Z-9.9958 I20.106 J-4.	N658 Y-29. Z-11.0591	N704 G01 X29. Z-12.0043
N608 G01 X29. Z-10.0043	N660 X-29. Z-11.114	N706 Y-29. Z-12.0591
N610 Y-29. Z-10.0591		
N612 X-29. Z-10.114		
N614 Y29. Z-10.1689		

N708 X-29. Z-12.114	N754 Y-29. Z-13.0591	N800 G01 X29. Z-14.0043
N710 Y29. Z-12.1689	N756 X-29. Z-13.114	N802 Y-29. Z-14.0591
N712 X-20.106 Z-12.1773	N758 Y29. Z-13.1689	N804 X-29. Z-14.114
N714 G03 X20.106 Y29. Z-12.2458 I20.106 J-4.	N760 X-20.106 Z-13.1773	N806 Y29. Z-14.1689
N716 G01 X29. Z-12.2543	N762 G03 X20.106 Y29. Z-13.2458 I20.106 J-4.	N808 X-20.106 Z-14.1773
N718 Y-29. Z-12.3091	N764 G01 X29. Z-13.2543	N810 G03 X20.106 Y29. Z-14.2458 I20.106 J-4.
N720 X-29. Z-12.364	N766 Y-29. Z-13.3091	N812 G01 X29. Z-14.2543
N722 Y29. Z-12.4189	N768 X-29. Z-13.364	N814 Y-29. Z-14.3091
N724 X-20.106 Z-12.4273	N770 Y29. Z-13.4189	N816 X-29. Z-14.364
N726 G03 X20.106 Y29. Z-12.4958 I20.106 J-4.	N772 X-20.106 Z-13.4273	N818 Y29. Z-14.4189
N728 G01 X29. Z-12.5043	N774 G03 X20.106 Y29. Z-13.4958 I20.106 J-4.	N820 X-20.106 Z-14.4273
N730 Y-29. Z-12.5591	N776 G01 X29. Z-13.5043	N822 G03 X20.106 Y29. Z-14.4958 I20.106 J-4.
N732 X-29. Z-12.614	N778 Y-29. Z-13.5591	N824 G01 X29. Z-14.5043
N734 Y29. Z-12.6689	N780 X-29. Z-13.614	N826 Y-29. Z-14.5591
N736 X-20.106 Z-12.6773	N782 Y29. Z-13.6689	N828 X-29. Z-14.614
N738 G03 X20.106 Y29. Z-12.7458 I20.106 J-4.	N784 X-20.106 Z-13.6773	N830 Y29. Z-14.6689
N740 G01 X29. Z-12.7543	N786 G03 X20.106 Y29. Z-13.7458 I20.106 J-4.	N832 X-20.106 Z-14.6773
N742 Y-29. Z-12.8091	N788 G01 X29. Z-13.7543	N834 G03 X20.106 Y29. Z-14.7458 I20.106 J-4.
N744 X-29. Z-12.864	N790 Y-29. Z-13.8091	N836 G01 X29. Z-14.7543
N746 Y29. Z-12.9189	N792 X-29. Z-13.864	N838 Y-29. Z-14.8091
N748 X-20.106 Z-12.9273	N794 Y29. Z-13.9189	N840 X-29. Z-14.864
N750 G03 X20.106 Y29. Z-12.9958 I20.106 J-4.	N796 X-20.106 Z-13.9273	N842 Y29. Z-14.9189
N752 G01 X29. Z-13.0043	N798 G03 X20.106 Y29. Z-13.9958 I20.106 J-4.	N844 X-20.106 Z-14.9273

N846 G03 X20.106 Y29. Z-14.9958 I20.106 J-4.	N892 X-20.106 Z- 15.9273	N938 Y29. Z-16.9189
N848 G01 X29. Z- 15.0043	N894 G03 X20.106 Y29. Z-15.9958 I20.106 J-4.	N940 X-20.106 Z- 16.9273
N850 Y-29. Z-15.0591	N896 G01 X29. Z- 16.0043	N942 G03 X20.106 Y29. Z-16.9958 I20.106 J-4.
N852 X-29. Z-15.114	N898 Y-29. Z-16.0591	N944 G01 X29. Z- 17.0043
N854 Y29. Z-15.1689	N900 X-29. Z-16.114	N946 Y-29. Z-17.0591
N856 X-20.106 Z- 15.1773	N902 Y29. Z-16.1689	N948 X-29. Z-17.114
N858 G03 X20.106 Y29. Z-15.2458 I20.106 J-4.	N904 X-20.106 Z- 16.1773	N950 Y29. Z-17.1689
N860 G01 X29. Z- 15.2543	N906 G03 X20.106 Y29. Z-16.2458 I20.106 J-4.	N952 X-20.106 Z- 17.1773
N862 Y-29. Z-15.3091	N908 G01 X29. Z- 16.2543	N954 G03 X20.106 Y29. Z-17.2458 I20.106 J-4.
N864 X-29. Z-15.364	N910 Y-29. Z-16.3091	N956 G01 X29. Z- 17.2543
N866 Y29. Z-15.4189	N912 X-29. Z-16.364	N958 Y-29. Z-17.3091
N868 X-20.106 Z- 15.4273	N914 Y29. Z-16.4189	N960 X-29. Z-17.364
N870 G03 X20.106 Y29. Z-15.4958 I20.106 J-4.	N916 X-20.106 Z- 16.4273	N962 Y29. Z-17.4189
N872 G01 X29. Z- 15.5043	N918 G03 X20.106 Y29. Z-16.4958 I20.106 J-4.	N964 X-20.106 Z- 17.4273
N874 Y-29. Z-15.5591	N920 G01 X29. Z- 16.5043	N966 G03 X20.106 Y29. Z-17.4958 I20.106 J-4.
N876 X-29. Z-15.614	N922 Y-29. Z-16.5591	N968 G01 X29. Z- 17.5043
N878 Y29. Z-15.6689	N924 X-29. Z-16.614	N970 Y-29. Z-17.5591
N880 X-20.106 Z- 15.6773	N926 Y29. Z-16.6689	N972 X-29. Z-17.614
N882 G03 X20.106 Y29. Z-15.7458 I20.106 J-4.	N928 X-20.106 Z- 16.6773	N974 Y29. Z-17.6689
N884 G01 X29. Z- 15.7543	N930 G03 X20.106 Y29. Z-16.7458 I20.106 J-4.	N976 X-20.106 Z- 17.6773
N886 Y-29. Z-15.8091	N932 G01 X29. Z- 16.7543	N978 G03 X20.106 Y29. Z-17.7458 I20.106 J-4.
N888 X-29. Z-15.864	N934 Y-29. Z-16.8091	N980 G01 X29. Z- 17.7543
N890 Y29. Z-15.9189	N936 X-29. Z-16.864	N982 Y-29. Z-17.8091

N984 X-29. Z-17.864	N1026 G03 X20.106 Y29. Z-18.7458 I20.106 J-4.	N1068 X-29. Z-19.614
N986 Y29. Z-17.9189	N1028 G01 X29. Z- 18.7543	N1070 Y29. Z-19.6689
N988 X-20.106 Z- 17.9273	N1030 Y-29. Z-18.8091	N1072 X-20.106 Z- 19.6773
N990 G03 X20.106 Y29. Z-17.9958 I20.106 J-4.	N1032 X-29. Z-18.864	N1074 G03 X20.106 Y29. Z-19.7458 I20.106 J-4.
N992 G01 X29. Z- 18.0043	N1034 Y29. Z-18.9189	N1076 G01 X29. Z- 19.7543
N994 Y-29. Z-18.0591	N1036 X-20.106 Z- 18.9273	N1078 Y-29. Z-19.8091
N996 X-29. Z-18.114	N1038 G03 X20.106 Y29. Z-18.9958 I20.106 J-4.	N1080 X-29. Z-19.864
N998 Y29. Z-18.1689	N1040 G01 X29. Z- 19.0043	N1082 Y29. Z-19.9189
N1000 X-20.106 Z- 18.1773	N1042 Y-29. Z-19.0591	N1084 X-20.106 Z- 19.9273
N1002 G03 X20.106 Y29. Z-18.2458 I20.106 J-4.	N1044 X-29. Z-19.114	N1086 G03 X20.106 Y29. Z-19.9958 I20.106 J-4.
N1004 G01 X29. Z- 18.2543	N1046 Y29. Z-19.1689	N1088 G01 X29. Z- 20.0043
N1006 Y-29. Z-18.3091	N1048 X-20.106 Z- 19.1773	N1090 Y-29. Z-20.0591
N1008 X-29. Z-18.364	N1050 G03 X20.106 Y29. Z-19.2458 I20.106 J-4.	N1092 X-29. Z-20.114
N1010 Y29. Z-18.4189	N1052 G01 X29. Z- 19.2543	N1094 Y29. Z-20.1689
N1012 X-20.106 Z- 18.4273	N1054 Y-29. Z-19.3091	N1096 X-20.106 Z- 20.1773
N1014 G03 X20.106 Y29. Z-18.4958 I20.106 J-4.	N1056 X-29. Z-19.364	N1098 G03 X20.106 Y29. Z-20.2458 I20.106 J-4.
N1016 G01 X29. Z- 18.5043	N1058 Y29. Z-19.4189	N1100 G01 X29. Z- 20.2543
N1018 Y-29. Z-18.5591	N1060 X-20.106 Z- 19.4273	N1102 Y-29. Z-20.3091
N1020 X-29. Z-18.614	N1062 G03 X20.106 Y29. Z-19.4958 I20.106 J-4.	N1104 X-29. Z-20.364
N1022 Y29. Z-18.6689	N1064 G01 X29. Z- 19.5043	N1106 Y29. Z-20.4189
N1024 X-20.106 Z- 18.6773	N1066 Y-29. Z-19.5591	N1108 X-20.106 Z- 20.4273

N1110 G03 X20.106
Y29. Z-20.4958 I20.106
J-4.

N1112 G01 X29. Z-
20.5043

N1114 Y-29. Z-20.5591

N1116 X-29. Z-20.614

N1118 Y29. Z-20.6689

N1120 X-20.106 Z-
20.6773

N1122 G03 X20.106
Y29. Z-20.7458 I20.106
J-4.

N1124 G01 X29. Z-
20.7543

N1126 Y-29. Z-20.8091

N1128 X-29. Z-20.864

N1130 Y29. Z-20.9189

N1132 X-20.106 Z-
20.9273

N1134 G03 X20.106
Y29. Z-20.9958 I20.106
J-4.

N1136 G01 X29. Z-
21.0043

N1138 Y-29. Z-21.0591

N1140 X-29. Z-21.114

N1142 Y29. Z-21.1689

N1144 X-20.106 Z-
21.1773

N1146 G03 X20.106
Y29. Z-21.2458 I20.106
J-4.

N1148 G01 X29. Z-
21.2543

N1150 Y-29. Z-21.3091

N1152 X-29. Z-21.364

N1154 Y29. Z-21.4189

N1156 X-20.106 Z-
21.4273

N1158 G03 X20.106
Y29. Z-21.4958 I20.106
J-4.

N1160 G01 X29. Z-
21.5043

N1162 Y-29. Z-21.5591

N1164 X-29. Z-21.614

N1166 Y29. Z-21.6689

N1168 X-20.106 Z-
21.6773

N1170 G03 X20.106
Y29. Z-21.7458 I20.106
J-4.

N1172 G01 X29. Z-
21.7543

N1174 Y-29. Z-21.8091

N1176 X-29. Z-21.864

N1178 Y29. Z-21.9189

N1180 X-20.106 Z-
21.9273

N1182 G03 X20.106
Y29. Z-21.9958 I20.106
J-4.

N1184 G01 X29. Z-
22.0043

N1186 Y-29. Z-22.0591

N1188 X-29. Z-22.114

N1190 Y29. Z-22.1689

N1192 X-20.106 Z-
22.1773

N1194 G03 X20.106
Y29. Z-22.2458 I20.106
J-4.

N1196 G01 X29. Z-
22.2543

N1198 Y-29. Z-22.3091

N1200 X-29. Z-22.364

N1202 Y29. Z-22.4189

N1204 X-20.106 Z-
22.4273

N1206 G03 X20.106
Y29. Z-22.4958 I20.106
J-4.

N1208 G01 X29. Z-
22.5043

N1210 Y-29. Z-22.5591

N1212 X-29. Z-22.614

N1214 Y29. Z-22.6689

N1216 X-20.106 Z-
22.6773

N1218 G03 X20.106
Y29. Z-22.7458 I20.106
J-4.

N1220 G01 X29. Z-
22.7543

N1222 Y-29. Z-22.8091

N1224 X-29. Z-22.864

N1226 Y29. Z-22.9189

N1228 X-20.106 Z-
22.9273

N1230 G03 X20.106
Y29. Z-22.9958 I20.106
J-4.

N1232 G01 X29. Z-
23.0043

N1234 Y-29. Z-23.0591

N1236 X-29. Z-23.114	N1278 G03 X20.106 Y29. Z-23.9958 I20.106 J-4.	N1320 X-29. Z-24.864
N1238 Y29. Z-23.1689	N1280 G01 X29. Z- 24.0043	N1322 Y29. Z-24.9189
N1240 X-20.106 Z- 23.1773	N1282 Y-29. Z-24.0591	N1324 X-20.106 Z- 24.9273
N1242 G03 X20.106 Y29. Z-23.2458 I20.106 J-4.	N1284 X-29. Z-24.114	N1326 G03 X20.106 Y29. Z-24.9958 I20.106 J-4.
N1244 G01 X29. Z- 23.2543	N1286 Y29. Z-24.1689	N1328 G01 X29. Z- 25.0043
N1246 Y-29. Z-23.3091	N1288 X-20.106 Z- 24.1773	N1330 Y-29. Z-25.0591
N1248 X-29. Z-23.364	N1290 G03 X20.106 Y29. Z-24.2458 I20.106 J-4.	N1332 X-29. Z-25.114
N1250 Y29. Z-23.4189	N1292 G01 X29. Z- 24.2543	N1334 Y29. Z-25.1689
N1252 X-20.106 Z- 23.4273	N1294 Y-29. Z-24.3091	N1336 X-20.106 Z- 25.1773
N1254 G03 X20.106 Y29. Z-23.4958 I20.106 J-4.	N1296 X-29. Z-24.364	N1338 G03 X20.106 Y29. Z-25.2458 I20.106 J-4.
N1256 G01 X29. Z- 23.5043	N1298 Y29. Z-24.4189	N1340 G01 X29. Z- 25.2543
N1258 Y-29. Z-23.5591	N1300 X-20.106 Z- 24.4273	N1342 Y-29. Z-25.3091
N1260 X-29. Z-23.614	N1302 G03 X20.106 Y29. Z-24.4958 I20.106 J-4.	N1344 X-29. Z-25.364
N1262 Y29. Z-23.6689	N1304 G01 X29. Z- 24.5043	N1346 Y29. Z-25.4189
N1264 X-20.106 Z- 23.6773	N1306 Y-29. Z-24.5591	N1348 X-20.106 Z- 25.4273
N1266 G03 X20.106 Y29. Z-23.7458 I20.106 J-4.	N1308 X-29. Z-24.614	N1350 G03 X20.106 Y29. Z-25.4958 I20.106 J-4.
N1268 G01 X29. Z- 23.7543	N1310 Y29. Z-24.6689	N1352 G01 X29. Z- 25.5043
N1270 Y-29. Z-23.8091	N1312 X-20.106 Z- 24.6773	N1354 Y-29. Z-25.5591
N1272 X-29. Z-23.864	N1314 G03 X20.106 Y29. Z-24.7458 I20.106 J-4.	N1356 X-29. Z-25.614
N1274 Y29. Z-23.9189	N1316 G01 X29. Z- 24.7543	N1358 Y29. Z-25.6689
N1276 X-20.106 Z- 23.9273	N1318 Y-29. Z-24.8091	N1360 X-20.106 Z- 25.6773

N1362 G03 X20.106
Y29. Z-25.7458 I20.106
J-4.

N1364 G01 X29. Z-
25.7543

N1366 Y-29. Z-25.8091

N1368 X-29. Z-25.864

N1370 Y29. Z-25.9189

N1372 X-20.106 Z-
25.9273

N1374 G03 X20.106
Y29. Z-25.9958 I20.106
J-4.

N1376 G01 X29. Z-
26.0043

N1378 Y-29. Z-26.0591

N1380 X-29. Z-26.114

N1382 Y29. Z-26.1689

N1384 X-20.106 Z-
26.1773

N1386 G03 X20.106
Y29. Z-26.2458 I20.106
J-4.

N1388 G01 X29. Z-
26.2543

N1390 Y-29. Z-26.3091

N1392 X-29. Z-26.364

N1394 Y29. Z-26.4189

N1396 X-20.106 Z-
26.4273

N1398 G03 X20.106
Y29. Z-26.4958 I20.106
J-4.

N1400 G01 X29. Z-
26.5043

N1402 Y-29. Z-26.5591

N1404 X-29. Z-26.614

N1406 Y29. Z-26.6689

N1408 X-20.106 Z-
26.6773

N1410 G03 X20.106
Y29. Z-26.7458 I20.106
J-4.

N1412 G01 X29. Z-
26.7543

N1414 Y-29. Z-26.8091

N1416 X-29. Z-26.864

N1418 Y29. Z-26.9189

N1420 X-20.106 Z-
26.9273

N1422 G03 X20.106
Y29. Z-26.9958 I20.106
J-4.

N1424 G01 X29. Z-
27.0043

N1426 Y-29. Z-27.0591

N1428 X-29. Z-27.114

N1430 Y29. Z-27.1689

N1432 X-20.106 Z-
27.1773

N1434 G03 X20.106
Y29. Z-27.2458 I20.106
J-4.

N1436 G01 X29. Z-
27.2543

N1438 Y-29. Z-27.3091

N1440 X-29. Z-27.364

N1442 Y29. Z-27.4189

N1444 X-20.106 Z-
27.4273

N1446 G03 X20.106
Y29. Z-27.4958 I20.106
J-4.

N1448 G01 X29. Z-
27.5043

N1450 Y-29. Z-27.5591

N1452 X-29. Z-27.614

N1454 Y29. Z-27.6689

N1456 X-20.106 Z-
27.6773

N1458 G03 X20.106
Y29. Z-27.7458 I20.106
J-4.

N1460 G01 X29. Z-
27.7543

N1462 Y-29. Z-27.8091

N1464 X-29. Z-27.864

N1466 Y29. Z-27.9189

N1468 X-20.106 Z-
27.9273

N1470 G03 X20.106
Y29. Z-27.9958 I20.106
J-4.

N1472 G01 X29. Z-
28.0043

N1474 Y-29. Z-28.0591

N1476 X-29. Z-28.114

N1478 Y29. Z-28.1689

N1480 X-20.106 Z-
28.1773

N1482 G03 X20.106
Y29. Z-28.2458 I20.106
J-4.

N1484 G01 X29. Z-
28.2543

N1486 Y-29. Z-28.3091

N1488 X-29. Z-28.364	N1530 G03 X20.106 Y29. Z-29.2458 I20.106 J-4.	N1572 X-29. Z-30.114
N1490 Y29. Z-28.4189	N1532 G01 X29. Z- 29.2543	N1574 Y29. Z-30.1689
N1492 X-20.106 Z- 28.4273	N1534 Y-29. Z-29.3091	N1576 X-20.106 Z- 30.1773
N1494 G03 X20.106 Y29. Z-28.4958 I20.106 J-4.	N1536 X-29. Z-29.364	N1578 G03 X20.106 Y29. Z-30.2458 I20.106 J-4.
N1496 G01 X29. Z- 28.5043	N1538 Y29. Z-29.4189	N1580 G01 X29. Z- 30.2543
N1498 Y-29. Z-28.5591	N1540 X-20.106 Z- 29.4273	N1582 Y-29. Z-30.3091
N1500 X-29. Z-28.614	N1542 G03 X20.106 Y29. Z-29.4958 I20.106 J-4.	N1584 X-29. Z-30.364
N1502 Y29. Z-28.6689	N1544 G01 X29. Z- 29.5043	N1586 Y29. Z-30.4189
N1504 X-20.106 Z- 28.6773	N1546 Y-29. Z-29.5591	N1588 X-20.106 Z- 30.4273
N1506 G03 X20.106 Y29. Z-28.7458 I20.106 J-4.	N1548 X-29. Z-29.614	N1590 G03 X20.106 Y29. Z-30.4958 I20.106 J-4.
N1508 G01 X29. Z- 28.7543	N1550 Y29. Z-29.6689	N1592 G01 X29. Z- 30.5043
N1510 Y-29. Z-28.8091	N1552 X-20.106 Z- 29.6773	N1594 Y-29. Z-30.5591
N1512 X-29. Z-28.864	N1554 G03 X20.106 Y29. Z-29.7458 I20.106 J-4.	N1596 X-29. Z-30.614
N1514 Y29. Z-28.9189	N1556 G01 X29. Z- 29.7543	N1598 Y29. Z-30.6689
N1516 X-20.106 Z- 28.9273	N1558 Y-29. Z-29.8091	N1600 X-20.106 Z- 30.6773
N1518 G03 X20.106 Y29. Z-28.9958 I20.106 J-4.	N1560 X-29. Z-29.864	N1602 G03 X20.106 Y29. Z-30.7458 I20.106 J-4.
N1520 G01 X29. Z- 29.0043	N1562 Y29. Z-29.9189	N1604 G01 X29. Z- 30.7543
N1522 Y-29. Z-29.0591	N1564 X-20.106 Z- 29.9273	N1606 Y-29. Z-30.8091
N1524 X-29. Z-29.114	N1566 G03 X20.106 Y29. Z-29.9958 I20.106 J-4.	N1608 X-29. Z-30.864
N1526 Y29. Z-29.1689	N1568 G01 X29. Z- 30.0043	N1610 Y29. Z-30.9189
N1528 X-20.106 Z- 29.1773	N1570 Y-29. Z-30.0591	N1612 X-20.106 Z- 30.9273

N1614 G03 X20.106
Y29. Z-30.9958 I20.106
J-4.

N1616 G01 X29. Z-
31.0043

N1618 Y-29. Z-31.0591

N1620 X-29. Z-31.114

N1622 Y29. Z-31.1689

N1624 X-20.106 Z-
31.1773

N1626 G03 X20.106
Y29. Z-31.2458 I20.106
J-4.

N1628 G01 X29. Z-
31.2543

N1630 Y-29. Z-31.3091

N1632 X-29. Z-31.364

N1634 Y29. Z-31.4189

N1636 X-20.106 Z-
31.4273

N1638 G03 X20.106
Y29. Z-31.4958 I20.106
J-4.

N1640 G01 X29. Z-
31.5043

N1642 Y-29. Z-31.5591

N1644 X-29. Z-31.614

N1646 Y29. Z-31.6689

N1648 X-20.106 Z-
31.6773

N1650 G03 X20.106
Y29. Z-31.7458 I20.106
J-4.

N1652 G01 X29. Z-
31.7543

N1654 Y-29. Z-31.8091

N1656 X-29. Z-31.864

N1658 Y29. Z-31.9189

N1660 X-20.106 Z-
31.9273

N1662 G03 X20.106
Y29. Z-31.9958 I20.106
J-4.

N1664 G01 X29. Z-
32.0043

N1666 Y-29. Z-32.0591

N1668 X-29. Z-32.114

N1670 Y29. Z-32.1689

N1672 X-20.106 Z-
32.1773

N1674 G03 X20.106
Y29. Z-32.2458 I20.106
J-4.

N1676 G01 X29. Z-
32.2543

N1678 Y-29. Z-32.3091

N1680 X-29. Z-32.364

N1682 Y29. Z-32.4189

N1684 X-20.106 Z-
32.4273

N1686 G03 X20.106
Y29. Z-32.4958 I20.106
J-4.

N1688 G01 X29. Z-
32.5043

N1690 Y-29. Z-32.5591

N1692 X-29. Z-32.614

N1694 Y29. Z-32.6689

N1696 X-20.106 Z-
32.6773

N1698 G03 X20.106
Y29. Z-32.7458 I20.106
J-4.

N1700 G01 X29. Z-
32.7543

N1702 Y-29. Z-32.8091

N1704 X-29. Z-32.864

N1706 Y29. Z-32.9189

N1708 X-20.106 Z-
32.9273

N1710 G03 X20.106
Y29. Z-32.9958 I20.106
J-4.

N1712 G01 X29. Z-
33.0043

N1714 Y-29. Z-33.0591

N1716 X-29. Z-33.114

N1718 Y29. Z-33.1689

N1720 X-20.106 Z-
33.1773

N1722 G03 X20.106
Y29. Z-33.2458 I20.106
J-4.

N1724 G01 X29. Z-
33.2543

N1726 Y-29. Z-33.3091

N1728 X-29. Z-33.364

N1730 Y29. Z-33.4189

N1732 X-20.106 Z-
33.4273

N1734 G03 X20.106
Y29. Z-33.4958 I20.106
J-4.

N1736 G01 X29. Z-
33.5043

N1738 Y-29. Z-33.5591

N1740 X-29. Z-33.614	N1782 G03 X20.106	N1824 X-29. Z-35.364
N1742 Y29. Z-33.6689	Y29. Z-34.4958 I20.106	N1826 Y29. Z-35.4189
N1744 X-20.106 Z-	J-4.	N1828 X-20.106 Z-
33.6773	N1784 G01 X29. Z-	35.4273
N1746 G03 X20.106	34.5043	N1830 G03 X20.106
Y29. Z-33.7458 I20.106	N1786 Y-29. Z-34.5591	Y29. Z-35.4958 I20.106
J-4.	N1788 X-29. Z-34.614	J-4.
N1748 G01 X29. Z-	N1790 Y29. Z-34.6689	N1832 G01 X29. Z-
33.7543	N1792 X-20.106 Z-	35.5043
N1750 Y-29. Z-33.8091	34.6773	N1834 Y-29. Z-35.5591
N1752 X-29. Z-33.864	N1794 G03 X20.106	N1836 X-29. Z-35.614
N1754 Y29. Z-33.9189	Y29. Z-34.7458 I20.106	N1838 Y29. Z-35.6689
N1756 X-20.106 Z-	J-4.	N1840 X-20.106 Z-
33.9273	N1796 G01 X29. Z-	35.6773
N1758 G03 X20.106	34.7543	N1842 G03 X20.106
Y29. Z-33.9958 I20.106	N1798 Y-29. Z-34.8091	Y29. Z-35.7458 I20.106
J-4.	N1800 X-29. Z-34.864	J-4.
N1760 G01 X29. Z-	N1802 Y29. Z-34.9189	N1844 G01 X29. Z-
34.0043	N1804 X-20.106 Z-	35.7543
N1762 Y-29. Z-34.0591	34.9273	N1846 Y-29. Z-35.8091
N1764 X-29. Z-34.114	N1806 G03 X20.106	N1848 X-29. Z-35.864
N1766 Y29. Z-34.1689	Y29. Z-34.9958 I20.106	N1850 Y29. Z-35.9189
N1768 X-20.106 Z-	J-4.	N1852 X-20.106 Z-
34.1773	N1808 G01 X29. Z-	35.9273
N1770 G03 X20.106	35.0043	N1854 G03 X20.106
Y29. Z-34.2458 I20.106	N1810 Y-29. Z-35.0591	Y29. Z-35.9958 I20.106
J-4.	N1812 X-29. Z-35.114	J-4.
N1772 G01 X29. Z-	N1814 Y29. Z-35.1689	N1856 G01 X29. Z-
34.2543	N1816 X-20.106 Z-	36.0043
N1774 Y-29. Z-34.3091	35.1773	N1858 Y-29. Z-36.0591
N1776 X-29. Z-34.364	N1818 G03 X20.106	N1860 X-29. Z-36.114
N1778 Y29. Z-34.4189	Y29. Z-35.2458 I20.106	N1862 Y29. Z-36.1689
N1780 X-20.106 Z-	J-4.	N1864 X-20.106 Z-
34.4273	N1820 G01 X29. Z-	36.1773
	35.2543	
	N1822 Y-29. Z-35.3091	

N1866 G03 X20.106
Y29. Z-36.2458 I20.106
J-4.

N1868 G01 X29. Z-
36.2543

N1870 Y-29. Z-36.3091

N1872 X-29. Z-36.364

N1874 Y29. Z-36.4189

N1876 X-20.106 Z-
36.4273

N1878 G03 X20.106
Y29. Z-36.4958 I20.106
J-4.

N1880 G01 X29. Z-
36.5043

N1882 Y-29. Z-36.5591

N1884 X-29. Z-36.614

N1886 Y29. Z-36.6689

N1888 X-20.106 Z-
36.6773

N1890 G03 X20.106
Y29. Z-36.7458 I20.106
J-4.

N1892 G01 X29. Z-
36.7543

N1894 Y-29. Z-36.8091

N1896 X-29. Z-36.864

N1898 Y29. Z-36.9189

N1900 X-20.106 Z-
36.9273

N1902 G03 X20.106
Y29. Z-36.9958 I20.106
J-4.

N1904 G01 X29. Z-
37.0043

N1906 Y-29. Z-37.0591

N1908 X-29. Z-37.114

N1910 Y29. Z-37.1689

N1912 X-20.106 Z-
37.1773

N1914 G03 X20.106
Y29. Z-37.2458 I20.106
J-4.

N1916 G01 X29. Z-
37.2543

N1918 Y-29. Z-37.3091

N1920 X-29. Z-37.364

N1922 Y29. Z-37.4189

N1924 X-20.106 Z-
37.4273

N1926 G03 X20.106
Y29. Z-37.4958 I20.106
J-4.

N1928 G01 X29. Z-
37.5043

N1930 Y-29. Z-37.5591

N1932 X-29. Z-37.614

N1934 Y29. Z-37.6689

N1936 X-20.106 Z-
37.6773

N1938 G03 X20.106
Y29. Z-37.7458 I20.106
J-4.

N1940 G01 X29. Z-
37.7543

N1942 Y-29. Z-37.8091

N1944 X-29. Z-37.864

N1946 Y29. Z-37.9189

N1948 X-20.106 Z-
37.9273

N1950 G03 X20.106
Y29. Z-37.9958 I20.106
J-4.

N1952 G01 X29. Z-
38.0043

N1954 Y-29. Z-38.0591

N1956 X-29. Z-38.114

N1958 Y29. Z-38.1689

N1960 X-20.106 Z-
38.1773

N1962 G03 X20.106
Y29. Z-38.2458 I20.106
J-4.

N1964 G01 X29. Z-
38.2543

N1966 Y-29. Z-38.3091

N1968 X-29. Z-38.364

N1970 Y29. Z-38.4189

N1972 X-20.106 Z-
38.4273

N1974 G03 X20.106
Y29. Z-38.4958 I20.106
J-4.

N1976 G01 X29. Z-
38.5043

N1978 Y-29. Z-38.5591

N1980 X-29. Z-38.614

N1982 Y29. Z-38.6689

N1984 X-20.106 Z-
38.6773

N1986 G03 X20.106
Y29. Z-38.7458 I20.106
J-4.

N1988 G01 X29. Z-
38.7543

N1990 Y-29. Z-38.8091

N1992 X-29. Z-38.864	N2034 G03 X20.106	N2076 X-29. Z-40.614
N1994 Y29. Z-38.9189	Y29. Z-39.7458 I20.106	N2078 Y29. Z-40.6689
N1996 X-20.106 Z-	J-4.	N2080 X-20.106 Z-
38.9273	N2036 G01 X29. Z-	40.6773
N1998 G03 X20.106	39.7543	N2082 G03 X20.106
Y29. Z-38.9958 I20.106	N2038 Y-29. Z-39.8091	Y29. Z-40.7458 I20.106
J-4.	N2040 X-29. Z-39.864	J-4.
N2000 G01 X29. Z-	N2042 Y29. Z-39.9189	N2084 G01 X29. Z-
39.0043	N2044 X-20.106 Z-	40.7543
N2002 Y-29. Z-39.0591	39.9273	N2086 Y-29. Z-40.8091
N2004 X-29. Z-39.114	N2046 G03 X20.106	N2088 X-29. Z-40.864
N2006 Y29. Z-39.1689	Y29. Z-39.9958 I20.106	N2090 Y29. Z-40.9189
N2008 X-20.106 Z-	J-4.	N2092 X-20.106 Z-
39.1773	N2048 G01 X29. Z-	40.9273
N2010 G03 X20.106	40.0043	N2094 G03 X20.106
Y29. Z-39.2458 I20.106	N2050 Y-29. Z-40.0591	Y29. Z-40.9958 I20.106
J-4.	N2052 X-29. Z-40.114	J-4.
N2012 G01 X29. Z-	N2054 Y29. Z-40.1689	N2096 G01 X29. Z-
39.2543	N2056 X-20.106 Z-	41.0043
N2014 Y-29. Z-39.3091	40.1773	N2098 Y-29. Z-41.0591
N2016 X-29. Z-39.364	N2058 G03 X20.106	N2100 X-29. Z-41.114
N2018 Y29. Z-39.4189	Y29. Z-40.2458 I20.106	N2102 Y29. Z-41.1689
N2020 X-20.106 Z-	J-4.	N2104 X-20.106 Z-
39.4273	N2060 G01 X29. Z-	41.1773
N2022 G03 X20.106	40.2543	N2106 G03 X20.106
Y29. Z-39.4958 I20.106	N2062 Y-29. Z-40.3091	Y29. Z-41.2458 I20.106
J-4.	N2064 X-29. Z-40.364	J-4.
N2024 G01 X29. Z-	N2066 Y29. Z-40.4189	N2108 G01 X29. Z-
39.5043	N2068 X-20.106 Z-	41.2543
N2026 Y-29. Z-39.5591	40.4273	N2110 Y-29. Z-41.3091
N2028 X-29. Z-39.614	N2070 G03 X20.106	N2112 X-29. Z-41.364
N2030 Y29. Z-39.6689	Y29. Z-40.4958 I20.106	N2114 Y29. Z-41.4189
N2032 X-20.106 Z-	J-4.	N2116 X-20.106 Z-
39.6773	N2072 G01 X29. Z-	41.4273
	40.5043	
	N2074 Y-29. Z-40.5591	

N2118 G03 X20.106 Y29. Z-41.4958 I20.106 J-4.	N2160 X-29. Z-42.364	N2202 G03 X20.106 Y29. Z-43.2458 I20.106 J-4.
N2120 G01 X29. Z- 41.5043	N2162 Y29. Z-42.4189	N2204 G01 X29. Z- 43.2543
N2122 Y-29. Z-41.5591	N2164 X-20.106 Z- 42.4273	N2206 Y-29. Z-43.3091
N2124 X-29. Z-41.614	N2166 G03 X20.106 Y29. Z-42.4958 I20.106 J-4.	N2208 X-29. Z-43.364
N2126 Y29. Z-41.6689	N2168 G01 X29. Z- 42.5043	N2210 Y29. Z-43.4189
N2128 X-20.106 Z- 41.6773	N2170 Y-29. Z-42.5591	N2212 X-20.106 Z- 43.4273
N2130 G03 X20.106 Y29. Z-41.7458 I20.106 J-4.	N2172 X-29. Z-42.614	N2214 G03 X20.106 Y29. Z-43.4958 I20.106 J-4.
N2132 G01 X29. Z- 41.7543	N2174 Y29. Z-42.6689	N2216 G01 X29. Z- 43.5043
N2134 Y-29. Z-41.8091	N2176 X-20.106 Z- 42.6773	N2218 Y-29. Z-43.5591
N2136 X-29. Z-41.864	N2178 G03 X20.106 Y29. Z-42.7458 I20.106 J-4.	N2220 X-29. Z-43.614
N2138 Y29. Z-41.9189	N2180 G01 X29. Z- 42.7543	N2222 Y29. Z-43.6689
N2140 X-20.106 Z- 41.9273	N2182 Y-29. Z-42.8091	N2224 X-20.106 Z- 43.6773
N2142 G03 X20.106 Y29. Z-41.9958 I20.106 J-4.	N2184 X-29. Z-42.864	N2226 G03 X20.106 Y29. Z-43.7458 I20.106 J-4.
N2144 G01 X29. Z- 42.0043	N2186 Y29. Z-42.9189	N2228 G01 X29. Z- 43.7543
N2146 Y-29. Z-42.0591	N2188 X-20.106 Z- 42.9273	N2230 Y-29. Z-43.8091
N2148 X-29. Z-42.114	N2190 G03 X20.106 Y29. Z-42.9958 I20.106 J-4.	N2232 X-29. Z-43.864
N2150 Y29. Z-42.1689	N2192 G01 X29. Z- 43.0043	N2234 Y29. Z-43.9189
N2152 X-20.106 Z- 42.1773	N2194 Y-29. Z-43.0591	N2236 X-20.106 Z- 43.9273
N2154 G03 X20.106 Y29. Z-42.2458 I20.106 J-4.	N2196 X-29. Z-43.114	N2238 G03 X20.106 Y29. Z-43.9958 I20.106 J-4.
N2156 G01 X29. Z- 42.2543	N2198 Y29. Z-43.1689	N2240 G01 X29. Z- 44.0043
N2158 Y-29. Z-42.3091	N2200 X-20.106 Z- 43.1773	N2242 Y-29. Z-44.0591

N2244 X-29. Z-44.114	N2286 G03 X20.106 Y29. Z-44.9958 I20.106 J-4.	N2328 X-29. Z-45.864
N2246 Y29. Z-44.1689	N2288 G01 X29. Z- 45.0043	N2330 Y29. Z-45.9189
N2248 X-20.106 Z- 44.1773	N2290 Y-29. Z-45.0591	N2332 X-20.106 Z- 45.9273
N2250 G03 X20.106 Y29. Z-44.2458 I20.106 J-4.	N2292 X-29. Z-45.114	N2334 G03 X20.106 Y29. Z-45.9958 I20.106 J-4.
N2252 G01 X29. Z- 44.2543	N2294 Y29. Z-45.1689	N2336 G01 X29. Z- 46.0043
N2254 Y-29. Z-44.3091	N2296 X-20.106 Z- 45.1773	N2338 Y-29. Z-46.0591
N2256 X-29. Z-44.364	N2298 G03 X20.106 Y29. Z-45.2458 I20.106 J-4.	N2340 X-29. Z-46.114
N2258 Y29. Z-44.4189	N2300 G01 X29. Z- 45.2543	N2342 Y29. Z-46.1689
N2260 X-20.106 Z- 44.4273	N2302 Y-29. Z-45.3091	N2344 X-20.106 Z- 46.1773
N2262 G03 X20.106 Y29. Z-44.4958 I20.106 J-4.	N2304 X-29. Z-45.364	N2346 G03 X20.106 Y29. Z-46.2458 I20.106 J-4.
N2264 G01 X29. Z- 44.5043	N2306 Y29. Z-45.4189	N2348 G01 X29. Z- 46.2543
N2266 Y-29. Z-44.5591	N2308 X-20.106 Z- 45.4273	N2350 Y-29. Z-46.3091
N2268 X-29. Z-44.614	N2310 G03 X20.106 Y29. Z-45.4958 I20.106 J-4.	N2352 X-29. Z-46.364
N2270 Y29. Z-44.6689	N2312 G01 X29. Z- 45.5043	N2354 Y29. Z-46.4189
N2272 X-20.106 Z- 44.6773	N2314 Y-29. Z-45.5591	N2356 X-20.106 Z- 46.4273
N2274 G03 X20.106 Y29. Z-44.7458 I20.106 J-4.	N2316 X-29. Z-45.614	N2358 G03 X20.106 Y29. Z-46.4958 I20.106 J-4.
N2276 G01 X29. Z- 44.7543	N2318 Y29. Z-45.6689	N2360 G01 X29. Z- 46.5043
N2278 Y-29. Z-44.8091	N2320 X-20.106 Z- 45.6773	N2362 Y-29. Z-46.5591
N2280 X-29. Z-44.864	N2322 G03 X20.106 Y29. Z-45.7458 I20.106 J-4.	N2364 X-29. Z-46.614
N2282 Y29. Z-44.9189	N2324 G01 X29. Z- 45.7543	N2366 Y29. Z-46.6689
N2284 X-20.106 Z- 44.9273	N2326 Y-29. Z-45.8091	N2368 X-20.106 Z- 46.6773

N2370 G03 X20.106
Y29. Z-46.7458 I20.106
J-4.

N2372 G01 X29. Z-
46.7543

N2374 Y-29. Z-46.8091

N2376 X-29. Z-46.864

N2378 Y29. Z-46.9189

N2380 X-20.106 Z-
46.9273

N2382 G03 X20.106
Y29. Z-46.9958 I20.106
J-4.

N2384 G01 X29. Z-
47.0043

N2386 Y-29. Z-47.0591

N2388 X-29. Z-47.114

N2390 Y29. Z-47.1689

N2392 X-20.106 Z-
47.1773

N2394 G03 X20.106
Y29. Z-47.2458 I20.106
J-4.

N2396 G01 X29. Z-
47.2543

N2398 Y-29. Z-47.3091

N2400 X-29. Z-47.364

N2402 Y29. Z-47.4189

N2404 X-20.106 Z-
47.4273

N2406 G03 X20.106
Y29. Z-47.4958 I20.106
J-4.

N2408 G01 X29. Z-
47.5043

N2410 Y-29. Z-47.5591

N2412 X-29. Z-47.614

N2414 Y29. Z-47.6689

N2416 X-20.106 Z-
47.6773

N2418 G03 X20.106
Y29. Z-47.7458 I20.106
J-4.

N2420 G01 X29. Z-
47.7543

N2422 Y-29. Z-47.8091

N2424 X-29. Z-47.864

N2426 Y29. Z-47.9189

N2428 X-20.106 Z-
47.9273

N2430 G03 X20.106
Y29. Z-47.9958 I20.106
J-4.

N2432 G01 X29. Z-
48.0043

N2434 Y-29. Z-48.0591

N2436 X-29. Z-48.114

N2438 Y29. Z-48.1689

N2440 X-20.106 Z-
48.1773

N2442 G03 X20.106
Y29. Z-48.2458 I20.106
J-4.

N2444 G01 X29. Z-
48.2543

N2446 Y-29. Z-48.3091

N2448 X-29. Z-48.364

N2450 Y29. Z-48.4189

N2452 X-20.106 Z-
48.4273

N2454 G03 X20.106
Y29. Z-48.4958 I20.106
J-4.

N2456 G01 X29. Z-
48.5043

N2458 Y-29. Z-48.5591

N2460 X-29. Z-48.614

N2462 Y29. Z-48.6689

N2464 X-20.106 Z-
48.6773

N2466 G03 X20.106
Y29. Z-48.7458 I20.106
J-4.

N2468 G01 X29. Z-
48.7543

N2470 Y-29. Z-48.8091

N2472 X-29. Z-48.864

N2474 Y29. Z-48.9189

N2476 X-20.106 Z-
48.9273

N2478 G03 X20.106
Y29. Z-48.9958 I20.106
J-4.

N2480 G01 X29. Z-
49.0043

N2482 Y-29. Z-49.0591

N2484 X-29. Z-49.114

N2486 Y29. Z-49.1689

N2488 X-20.106 Z-
49.1773

N2490 G03 X20.106
Y29. Z-49.2458 I20.106
J-4.

N2492 G01 X29. Z-
49.2543

N2494 Y-29. Z-49.3091

N2496 X-29. Z-49.364

N2498 Y29. Z-49.4189

N2500 X-20.106 Z-
49.4273

N2502 G03 X20.106
Y29. Z-49.4958 I20.106
J-4.

N2504 G01 X29. Z-
49.5043

N2506 Y-29. Z-49.5591

N2508 X-29. Z-49.614

N2510 Y29. Z-49.6689

N2512 X-20.106 Z-
49.6773

N2514 G03 X20.106
Y29. Z-49.7458 I20.106
J-4.

N2516 G01 X29. Z-
49.7543

N2518 Y-29. Z-49.8091

N2520 X-29. Z-49.864

N2522 Y29. Z-49.9189

N2524 X-20.106 Z-
49.9273

N2526 G03 X20.106
Y29. Z-49.9958 I20.106
J-4.

N2528 G01 X24.5 Z-50.

N2530 X29.

N2532 Y-29.

N2534 X-29.

N2536 Y29.

N2538 X-20.106

N2540 G03 X20.106
Y29. I20.106 J-4.

N2542 G01 X25.

N2544 G03 X31. Y35. I0.
J6.

N2546 G01 G40 X30.749

N2548 G00 Z25.

N2550 M05

N2552 G00 G28 G91 Z0

N2554 G00 G28 G91 X-
15.0 Y0.

N2556 G90

N2558 M06 T1

N2560 M30

%

Annexure 2

<hr/> <hr/> Program Name: Direct measure Inspection: 0 <hr/> Creation Date: 20-12-2017								
Creation Time: 11:47:03								
Circle1				<i>Circle.Measured</i>				
RefSys:		<i>MCS</i>						
	<i>Mea</i>	<i>Nom</i>	<i>Dev</i>	<i>Up</i>	<i>Low</i>	<i>UCrit</i>	<i>LCrit</i>	<i>Oot/Crit</i>
X	227.8241	227.8241	0.0000					
Y	198.5298	198.5298	0.0000					
Z	110.3224	110.3224	0.0000					
DIAM	50.0678	50.0678	0.0000					
CIRLTY	0.0000	0.0000	0.0000					
SIGMA	0.0000	0.0000	0.0000					
Circle2				<i>Circle.Measured</i>				
RefSys:		<i>MCS</i>						
	<i>Mea</i>	<i>Nom</i>	<i>Dev</i>	<i>Up</i>	<i>Low</i>	<i>UCrit</i>	<i>LCrit</i>	<i>Oot/Crit</i>
X	228.0876	228.0876	0.0000					
Y	198.5484	198.5484	0.0000					
Z	110.3925	110.3925	0.0000					
DIAM	50.2961	50.2961	0.0000					
CIRLTY	0.0000	0.0000	0.0000					
SIGMA	0.0000	0.0000	0.0000					
Point1				<i>Point.Measured</i>				
RefSys:		<i>MCS</i>						
	<i>Mea</i>	<i>Nom</i>	<i>Dev</i>	<i>Up</i>	<i>Low</i>	<i>UCrit</i>	<i>LCrit</i>	<i>Oot/Crit</i>
X	226.8523	226.8523	0.0000					
Y	231.5374	231.5374	0.0000					
Z	82.8202	82.8202	0.0000					
Point2				<i>Point.Measured</i>				
RefSys:		<i>MCS</i>						
	<i>Mea</i>	<i>Nom</i>	<i>Dev</i>	<i>Up</i>	<i>Low</i>	<i>UCrit</i>	<i>LCrit</i>	<i>Oot/Crit</i>
X	226.8540	226.8540	0.0000					
Y	186.7201	186.7201	0.0000					
Z	83.3632	83.3632	0.0000					
Distance1				<i>Distance</i>				
RefSys:		<i>MCS</i>						
	<i>Mea</i>	<i>Nom</i>	<i>Dev</i>	<i>Up</i>	<i>Low</i>	<i>UCrit</i>	<i>LCrit</i>	<i>Oot/Crit</i>

DISTB	44.8206	44.8206	0.0000					
DISTX	0.0017	0.0017	0.0000					
DISTY	44.8173	44.8173	0.0000					
DISTZ	0.5430	0.5430	0.0000					
Point3			<i>Point.Measured</i>					
RefSys:		MCS						
	<i>Mea</i>	<i>Nom</i>	<i>Dev</i>	<i>Up</i>	<i>Low</i>	<i>UCrit</i>	<i>LCrit</i>	<i>Oot/Crit</i>
X	226.8513	226.8513	0.0000					
Y	233.1411	233.1411	0.0000					
Z	106.1335	106.1335	0.0000					
Point4			<i>Point.Measured</i>					
RefSys:		MCS						
	<i>Mea</i>	<i>Nom</i>	<i>Dev</i>	<i>Up</i>	<i>Low</i>	<i>UCrit</i>	<i>LCrit</i>	<i>Oot/Crit</i>
X	226.8537	226.8537	0.0000					
Y	183.3351	183.3351	0.0000					
Z	106.1269	106.1269	0.0000					
Distance2			<i>Distance</i>					
RefSys:		MCS						
	<i>Mea</i>	<i>Nom</i>	<i>Dev</i>	<i>Up</i>	<i>Low</i>	<i>UCrit</i>	<i>LCrit</i>	<i>Oot/Crit</i>
DISTB	49.8060	49.8060	0.0000					
DISTX	0.0024	0.0024	0.0000					
DISTY	49.8060	49.8060	0.0000					
DISTZ	0.0066	0.0066	0.0000					
Point5			<i>Point.Measured</i>					
RefSys:		MCS						
	<i>Mea</i>	<i>Nom</i>	<i>Dev</i>	<i>Up</i>	<i>Low</i>	<i>UCrit</i>	<i>LCrit</i>	<i>Oot/Crit</i>
X	226.8515	226.8515	0.0000					
Y	232.9114	232.9114	0.0000					
Z	109.5067	109.5067	0.0000					
Point6			<i>Point.Measured</i>					
RefSys:		MCS						
	<i>Mea</i>	<i>Nom</i>	<i>Dev</i>	<i>Up</i>	<i>Low</i>	<i>UCrit</i>	<i>LCrit</i>	<i>Oot/Crit</i>
X	226.8538	226.8538	0.0000					
Y	183.8003	183.8003	0.0000					
Z	109.5015	109.5015	0.0000					
Distance3			<i>Distance</i>					
RefSys:		MCS						
	<i>Mea</i>	<i>Nom</i>	<i>Dev</i>	<i>Up</i>	<i>Low</i>	<i>UCrit</i>	<i>LCrit</i>	<i>Oot/Crit</i>
DISTB	49.1111	49.1111	0.0000					
DISTX	0.0023	0.0023	0.0000					

DISTY	49.1111	49.1111	0.0000					
DISTZ	0.0052	0.0052	0.0000					
Circle3			<i>Circle.Measured</i>					
RefSys:		<i>MCS</i>						
	<i>Mea</i>	<i>Nom</i>	<i>Dev</i>	<i>Up</i>	<i>Low</i>	<i>UCrit</i>	<i>LCrit</i>	<i>Oot/Crit</i>
X	212.6142	212.6142	0.0000					
Y	181.8808	181.8808	0.0000					
Z	135.0553	135.0553	0.0000					
DIAM	9.3660	9.3660	0.0000					
CIRLTY	0.0000	0.0000	0.0000					
SIGMA	0.0000	0.0000	0.0000					
Circle4			<i>Circle.Measured</i>					
RefSys:		<i>MCS</i>						
	<i>Mea</i>	<i>Nom</i>	<i>Dev</i>	<i>Up</i>	<i>Low</i>	<i>UCrit</i>	<i>LCrit</i>	<i>Oot/Crit</i>
X	232.3481	232.3481	0.0000					
Y	181.8799	181.8799	0.0000					
Z	134.9221	134.9221	0.0000					
DIAM	9.5386	9.5386	0.0000					
CIRLTY	0.0000	0.0000	0.0000					
SIGMA	0.0000	0.0000	0.0000					
Circle5			<i>Circle.Measured</i>					
RefSys:		<i>MCS</i>						
	<i>Mea</i>	<i>Nom</i>	<i>Dev</i>	<i>Up</i>	<i>Low</i>	<i>UCrit</i>	<i>LCrit</i>	<i>Oot/Crit</i>
X	252.2016	252.2016	0.0000					
Y	181.8801	181.8801	0.0000					
Z	134.6853	134.6853	0.0000					
DIAM	9.8771	9.8771	0.0000					
CIRLTY	0.0000	0.0000	0.0000					
SIGMA	0.0000	0.0000	0.0000					
Circle6			<i>Circle.Measured</i>					
RefSys:		<i>MCS</i>						
	<i>Mea</i>	<i>Nom</i>	<i>Dev</i>	<i>Up</i>	<i>Low</i>	<i>UCrit</i>	<i>LCrit</i>	<i>Oot/Crit</i>
X	222.4981	222.4981	0.0000					
Y	181.8801	181.8801	0.0000					
Z	134.8554	134.8554	0.0000					
DIAM	9.5238	9.5238	0.0000					
CIRLTY	0.0000	0.0000	0.0000					
SIGMA	0.0000	0.0000	0.0000					
Circle7			<i>Circle.Measured</i>					
RefSys:		<i>MCS</i>						

	<i>Mea</i>	<i>Nom</i>	<i>Dev</i>	<i>Up</i>	<i>Low</i>	<i>UCrit</i>	<i>LCrit</i>	<i>Oot/Crit</i>
X	242.1805	242.1805	0.0000					
Y	181.8802	181.8802	0.0000					
Z	134.9767	134.9767	0.0000					
DIAM	9.8618	9.8618	0.0000					
CIRLTY	0.0000	0.0000	0.0000					
SIGMA	0.0000	0.0000	0.0000					
Point7								<i>Point.Measured</i>
RefSys:		<i>MCS</i>						
	<i>Mea</i>	<i>Nom</i>	<i>Dev</i>	<i>Up</i>	<i>Low</i>	<i>UCrit</i>	<i>LCrit</i>	<i>Oot/Crit</i>
X	232.4018	232.4018	0.0000					
Y	210.0672	210.0672	0.0000					
Z	138.8489	138.8489	0.0000					
Point8								<i>Point.Measured</i>
RefSys:		<i>MCS</i>						
	<i>Mea</i>	<i>Nom</i>	<i>Dev</i>	<i>Up</i>	<i>Low</i>	<i>UCrit</i>	<i>LCrit</i>	<i>Oot/Crit</i>
X	232.4029	232.4029	0.0000					
Y	165.7645	165.7645	0.0000					
Z	138.8659	138.8659	0.0000					
Distance4								<i>Distance</i>
RefSys:		<i>MCS</i>						
	<i>Mea</i>	<i>Nom</i>	<i>Dev</i>	<i>Up</i>	<i>Low</i>	<i>UCrit</i>	<i>LCrit</i>	<i>Oot/Crit</i>
DISTB	44.3027	44.3027	0.0000					
DISTX	0.0012	0.0012	0.0000					
DISTY	44.3027	44.3027	0.0000					
DISTZ	0.0170	0.0170	0.0000					
Point9								<i>Point.Measured</i>
RefSys:		<i>MCS</i>						
	<i>Mea</i>	<i>Nom</i>	<i>Dev</i>	<i>Up</i>	<i>Low</i>	<i>UCrit</i>	<i>LCrit</i>	<i>Oot/Crit</i>
X	207.6264	207.6264	0.0000					
Y	191.2932	191.2932	0.0000					
Z	131.7262	131.7262	0.0000					
Point10								<i>Point.Measured</i>
RefSys:		<i>MCS</i>						
	<i>Mea</i>	<i>Nom</i>	<i>Dev</i>	<i>Up</i>	<i>Low</i>	<i>UCrit</i>	<i>LCrit</i>	<i>Oot/Crit</i>
X	257.0531	257.0531	0.0000					
Y	191.2932	191.2932	0.0000					
Z	131.7362	131.7362	0.0000					
Distance5								<i>Distance</i>
RefSys:		<i>MCS</i>						

	<i>Mea</i>	<i>Nom</i>	<i>Dev</i>	<i>Up</i>	<i>Low</i>	<i>UCrit</i>	<i>LCrit</i>	<i>Oot/Crit</i>
DISTB	49.4268	49.4268	0.0000					
DISTX	49.4267	49.4267	0.0000					
DISTY	0.0000	0.0000	0.0000					
DISTZ	0.0100	0.0100	0.0000					
<i>Point11</i>								<i>Point.Measured</i>
<i>RefSys:</i>		<i>MCS</i>						
	<i>Mea</i>	<i>Nom</i>	<i>Dev</i>	<i>Up</i>	<i>Low</i>	<i>UCrit</i>	<i>LCrit</i>	<i>Oot/Crit</i>
X	232.6512	232.6512	0.0000					
Y	219.3254	219.3254	0.0000					
Z	148.8306	148.8306	0.0000					
<i>Point12</i>								<i>Point.Measured</i>
<i>RefSys:</i>		<i>MCS</i>						
	<i>Mea</i>	<i>Nom</i>	<i>Dev</i>	<i>Up</i>	<i>Low</i>	<i>UCrit</i>	<i>LCrit</i>	<i>Oot/Crit</i>
X	232.6526	232.6526	0.0000					
Y	184.8112	184.8112	0.0000					
Z	148.8320	148.8320	0.0000					
<i>Distance6</i>								<i>Distance</i>
<i>RefSys:</i>		<i>MCS</i>						
	<i>Mea</i>	<i>Nom</i>	<i>Dev</i>	<i>Up</i>	<i>Low</i>	<i>UCrit</i>	<i>LCrit</i>	<i>Oot/Crit</i>
DISTB	34.5142	34.5142	0.0000					
DISTX	0.0014	0.0014	0.0000					
DISTY	34.5142	34.5142	0.0000					
DISTZ	0.0014	0.0014	0.0000					

Ish Thesis

ORIGINALITY REPORT

11 %	7 %	5 %	8 %
SIMILARITY INDEX	INTERNET SOURCES	PUBLICATIONS	STUDENT PAPERS

PRIMARY SOURCES

1	Submitted to Thapar University, Patiala Student Paper	1 %
2	www.platinumgmat.com Internet Source	1 %
3	nptel.ac.in Internet Source	1 %
4	en.wikipedia.org Internet Source	1 %
5	materialise.net Internet Source	1 %
6	www.stratasys.com Internet Source	1 %
7	Submitted to University of Birmingham Student Paper	<1 %
8	sffsymposium.engr.utexas.edu Internet Source	<1 %
9	Submitted to University Tun Hussein Onn Malaysia	<1 %

10

Submitted to University of Maryland, University College

Student Paper

<1 %

11

Submitted to DeVry University Online

Student Paper

<1 %

12

Submitted to University Centre Peterborough

Student Paper

<1 %

13

Mishra, Swayam Bikash, and Siba Sankar Mahapatra. "Improvement in Tensile Strength of FDM Built Parts by Parametric Control", Applied Mechanics and Materials, 2014.

Publication

<1 %

14

Submitted to University of Brighton

Student Paper

<1 %

15

Submitted to Burnley College, Lancashire

Student Paper

<1 %

16

www.ukessays.com

Internet Source

<1 %

17

S.H. Masood. "Advances in Fused Deposition Modeling", Elsevier BV, 2014

Publication

<1 %

18

academicromatic.net

Internet Source

<1 %

Submitted to Dublin City University